



CESPU

INSTITUTO UNIVERSITÁRIO
DE CIÊNCIAS DA SAÚDE

Deleterious effects of gadolinium in the proximal tubule: potential risks from the use of gadolinium-based contrast agents

Clique ou toque aqui para introduzir texto.

NÍCIA JUELMA DOS REIS SOUSA

Tese conducente ao Grau de Mestre em Ciências e Técnicas Laboratoriais Forenses

Gandra, outubro de 2021



CESPU

INSTITUTO UNIVERSITÁRIO
DE CIÊNCIAS DA SAÚDE

Nícia Juelma dos Reis Sousa

**Tese conducente ao Grau de Mestre em Ciências e Técnicas Laboratoriais
Forenses**

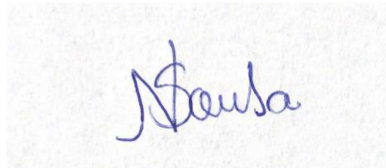
Deleterious effects of gadolinium in the proximal tubule: potential risks from the use of gadolinium- based contrast agents

Clique ou toque aqui para introduzir texto.

**Trabalho realizado sob a Orientação de Susana Coimbra, Maria João Valente e
Alice Santos-Silva**

Declaração de Integridade

Eu, acima identificado, declaro ter atuado com absoluta integridade na elaboração deste trabalho, confirmo que em todo o trabalho conducente à sua elaboração não recorri a qualquer forma de falsificação de resultados ou à prática de plágio (ato pelo qual um indivíduo, mesmo por omissão, assume a autoria do trabalho intelectual pertencente a outrem, na sua totalidade ou em partes dele). Mais declaro que todas as frases que retirei de trabalhos anteriores pertencentes a outros autores foram referenciadas ou redigidas com novas palavras, tendo neste caso colocado a citação da fonte bibliográfica.



Alcusa

To my parents
Manuela Reis e Joaquim R. de Sousa Júnior

Scientific communications in congress in poster or oral form

- **Poster**

- Reis Sousa NJ, Valente MJ, Santos-Silva A, Coimbra S. Nefrotoxicidade de agentes de contraste à base de gadolínio - avaliação dos mecanismos de toxicidade induzidos pelo gadolínio em células tubulares proximais humanas (HK-2). V Congresso da Associação Portuguesa de Ciências Forenses, XIV Jornadas Científicas de Ciências do IUCS, 2020.

- **Mini-oral**

- Reis Sousa N, Santos-Silva A, Coimbra S, Valente MJ. Nephrotoxic mechanisms of gadolinium: implications for the use of gadolinium-based contrast agents. 58th ERA-EDTA Congress, 5 - 8 july, 2021 (fully virtual).

Scientific production

- **Articles in international journals with scientific arbitration**
 - Reis Sousa, N., Rocha, S., Santos-Silva, A., Coimbra, S., & Valente, MJ. Cellular and molecular pathways underlying the nephrotoxicity of gadolinium. Submitted to *Toxicological Sciences*. Under review.

- **Communications in international journals with scientific arbitration**
 - Reis Sousa, N., Santos-Silva, A., Coimbra, S., & Valente MJ. (2021). Nephrotoxic mechanisms of gadolinium: implications for the use of gadolinium-based contrast agents. *Nephrol Dial Transplant* 36 (Supplement 1). DOI: 10.1093/ndt/gfab079.004
 - Abstract selected from ERA-EDTA 2021 Congress, published as: Reis Sousa, N., Santos-Silva, A., Coimbra, S., & Valente, MJ. (2021). Nephrotoxic Mechanisms of Gadolinium: Implications for the Use of Gadolinium-Based Contrast Agents. *EMJ Nephrology* 9.1: 46-47. Abstract Review No. AR1.

Agradecimentos

“O sucesso não consiste em não errar, mas em não cometer os mesmos equívocos mais de uma vez”.

George Bernard Shaw

Após um percurso exaustivo, longe do meu País e da família, vejo por concluído mais uma etapa da minha vida. Estes dois anos de formação foram de árdua jornada, desafios e ganhos de experiência. O presente trabalho não teria tomado um bom rumo sem o apoio e paciência de várias pessoas.

Agradeço a Deus em primeiro lugar.

Em especial agradeço as minhas orientadoras Susana Coimbra, Maria João Valente, Alice Santos-Silva por aceitarem o desafio de trabalhar comigo e pela sua incessável paciência, empenho e praticidade com que me orientaram durante o percurso do trabalho. Um agradecimento especial a Maria João Valente por sempre me motivar e corrigir-me quando necessário.

Agradeço também a Susana Rocha pelo apoio e a professora Mariele Luís por toda orientação ao longo do meu percurso académico e profissional.

Agradeço de igual modo ao Instituto Superior Politécnico de Benguela (ISPB) e ao Instituto Universitário de Ciências da Saúde — Cooperativa De Ensino Superior Politécnico e Universitário (IUCS-CESPU) pela oportunidade que me foi concedida. Um sincero agradecimento ao corpo docente desta faculdade pelos ensinamentos e pela infinita paciência. Gratifico também à Faculdade de Farmácia de Universidade de Porto por permitir a execução do trabalho no seu estabelecimento.

Por último, agradeço ao meu pai, Sousa Júnior, minha estrelinha, pois sei que onde quer que estejas cuidas de mim, à minha mãe, Manuela Reis, por tudo na vida, ao meu irmão Bridy Sousa e Margaret Sousa e aos meus amigos e colegas por me apoiarem e nunca me deixarem faltar nada.

Resumo

Os agentes de contraste que contêm gadolínio [Gd (III)] são utilizados há mais de 3 décadas, permitindo melhorar a qualidade e especificidade das imagens obtidas por ressonância magnética, usada no diagnóstico e monitorização do tratamento de diferentes patologias. Inicialmente considerados biologicamente inertes, estudos recentes têm demonstrado que o Gd (III) se liberta destes agentes e deposita-se em diferentes tecidos, causando toxicidade a curto e a médio prazo quando entra de novo em circulação. A via de excreção da maioria destes agentes é renal, e tem sido descrita uma toxicidade exacerbada em doentes renais, podendo mesmo conduzir ao desenvolvimento de fibrose nefrogénica sistémica, uma complicação grave e muitas vezes fatal, que resulta da libertação a longo prazo do Gd (III). Apesar das evidências de bioacumulação de Gd (III) e dos seus efeitos tóxicos, os mecanismos subjacentes à sua toxicidade, particularmente à nefrotoxicidade, são ainda pouco conhecidos.

Este trabalho teve como objetivo avaliar os mecanismos celulares e moleculares de nefrotoxicidade do Gd (III), utilizando um modelo *in vitro* de células tubulares proximais humanas (linha celular HK-2).

Observou-se diminuição da viabilidade celular de forma dependente da concentração e do tempo de exposição ao Gd (III). As concentrações inibitórias (CIs) que provocam 1 a 50 % de morte celular, após 24 horas de exposição, oscilaram entre 3,4 e 340,5 μ M. Nas concentrações tóxicas, a exposição ao Gd (III) desencadeou alterações no equilíbrio redox, disfunção mitocondrial, morte celular por apoptose, necrose nas concentrações mais altas, e ativação autofágica. Para CIs de baixa toxicidade observou-se perturbação do metabolismo lipídico, com acumulação de vesículas lipídicas, e desregulação de genes relacionados com a lipogénese e a lipólise. A exposição ao Gd (III), mesmo a um nível subtóxico, promoveu um aumento da expressão de marcadores envolvidos em várias vias de sinalização associadas com o desenvolvimento de inflamação, hipoxia e fibrose.

Mesmo a baixas concentrações, o Gd (III) pode desencadear uma resposta complexa e nociva nas células do túbulo proximal renal, com envolvimento de múltiplos fatores de risco comuns ao desenvolvimento e progressão de doença renal. É por isso crucial reavaliar o balanço entre os riscos e benefícios de exposição a este tipo de agentes de contraste, quer na população geral, quer nos doentes renais em particular.

Palavras-chave: gadolínio; nefrotoxicidade; stress oxidativo; disfunção mitocondrial; inflamação; deposição lipídica.

Abstract

Gadolinium [Gd (III)]-based contrast agents (GBCA) have been used for more than 30 years to improve the quality and specificity of magnetic resonance imaging, a crucial tool for medical diagnosis and treatment monitoring across multiple clinical settings. Initially considered biologically inert, recent studies have demonstrated that Gd (III) dechelates from these agents and undergoes tissue deposition in several organs, causing short- and long-term toxicity when released back into circulation. Most GBCA are excreted by the kidney, and exacerbated toxicity has been described in renal patients, sometimes leading to the development of nephrogenic systemic fibrosis. This is a severe complication, often fatal, associated to the long-term release of free Gd (III) from tissues in renal patients. Despite observations of the bioaccumulation of Gd (III) and its deleterious effects, data on Gd (III) toxicity mechanisms, particularly nephrotoxicity, are still relatively scarce.

This study aimed at unveiling the cellular and molecular mechanisms of nephrotoxicity of Gd (III), using an *in vitro* model of human proximal tubular cells (HK-2 cell line).

According to our results, cell viability declined in a concentration- and time-dependent manner after exposure to Gd (III). The estimated inhibitory concentrations (ICs) eliciting 1 to 50 % of cell death, after 24 h of exposure, ranged from 3.4 to 340.5 μM . At toxic concentrations, exposure to Gd (III) led to disruption of the redox status, mitochondrial dysfunction, cell death by apoptosis, switching to necrosis at higher levels, and autophagic activation. Disturbance of the lipid metabolism was already observed at low-toxicity ICs, with accumulation of lipid droplets, and upregulation of genes related to both lipogenesis and lipolysis. Gd (III)-exposure, even at the subtoxic IC_{01} , increased the expression of modulators of various signalling pathways involved in the development and progression of renal disease, including inflammation, hypoxia and fibrosis.

This work showed that, even at low levels, Gd (III) has the potential to trigger an intricate and deleterious response in the renal proximal tubule, that encompasses multiple risk factors that are known to underlie the development and progression of renal disease. It is crucial to reassess the balance between the risks and benefits of the exposure to GBCA, both in the general population and particularly in renal patients.

Keywords: Gadolinium; nephrotoxicity; oxidative stress; mitochondrial dysfunction; inflammation; lipid deposition.

Contents

Scientific communications in congress in poster or oral form	vi
Scientific production	vii
Agradecimentos	x
Resumo	xi
Abstract	xii
Figure contents	xiv
List of abbreviations	xv
I. Introduction	1
Historical background	2
Gadolinium complexes	3
GBCA pharmacokinetics and Gd (III) tissue deposition	5
General adverse effects	7
Renal toxicity and adverse effects in renal failure	9
Mechanisms of toxicity – <i>in vivo</i> and <i>in vitro</i> studies	11
Regulatory actions for GBCA use	13
II. Aims	15
III. Experimental Work	17
IV. Concluding Remarks and Future Perspectives	50
V. References	54

Figure contents

- Figure 1: Chemical structures of linear and macrocyclic gadolinium-based contrast agents, brand names and registering pharmaceutical companies. 4
- Figure 2: Process of dechelation (transmetallation) of Gd (III) from GBCA by endogenous cations. Substituted chelates are excreted from the organism. Ionic Gd (III) can precipitate in the presence of endogenous anionic molecules, and deposit in different tissues. 7
- Figure 3: Schematic view of the deleterious effects of gadolinium in the human proximal tubular cells. 52

List of abbreviations

ACACA: Acetyl-CoA carboxylase 1

ATP: Adenosine triphosphate

Bcl-2: B-cell lymphoma 2

Bmal1: Brain and muscle aryl hydrocarbon receptor nuclear translocator-like protein 1

CASP3: Caspase-3

CPT1A: Carnitine palmitoytransferase 1A

DMEM/F12: Dulbecco's Modified Eagle Medium/Nutrient Mixture F-12

DTNB: 5,5'-dithiobis (2-nitrobenzoic acid)

DTPA: Diethylenetriamine penta-acetic acid

EDTA: Ethylenediamine tetraacetic acid

EMA: European Medicines Agency

FBS: Fetal bovine serum

GBCA: Gadolinium-based contrast agents

GSH: L-glutathione reduced

GSSH: L-glutathione oxidized

HIF1A/HIF-1 α : Hypoxia-inducible factor-1 alpha

Hoechst 33342: bisBenzimide H 33342 trihydrochloride

IC: Inhibitory concentration

IL1B/IL-1 β : Interleukin-1 beta

IL6: Interleukin-6

LDH: Lactate dehydrogenase

mPTP: Mitochondrial permeability transition pore

MRI: Magnetic resonance imaging

MTT: Thiazolyl blue tetrazolium bromide

NFKB1: Nuclear factor-kappa B subunit 1

NF κ B: nuclear factor-kappa B

NRF2: Nuclear factor erythroid-2-related factor 2

NSF: nephrogenic systemic fibrosis

OPN/OPN: Osteopontin

PBS: Phosphate-buffered saline

PI: Propidium iodide

PRAC: Pandemic Response Accountability Committee



qPCR: Quantitative polymerase chain reaction

RES: Reticuloendothelial system

ROS: Reactive oxygen species

SQSTM1: Sequestosome-1

TAS: Total antioxidant status

TGFBI/ TGF- β : Transforming growth factor beta 1

tGSH: Total glutathione

TMRE: tetramethylrhodamine ethyl ester perchlorate

TPTZ: 2,3,5-triphenyltetrazolium chloride

β -NADPH: β -nicotinamide adenine dinucleotide 2'-phosphate reduced tetrasodium salt hydrate

$\Delta\Psi_m$: Mitochondrial membrane potential

I. Introduction

Historical background

Gadolinium [Gd (III)] is a rare-earth metal of the *lanthanide* series, atomic number 64, group 19 of the periodic table. In 1880, the Swiss chemist Jean Charles Galissard de Marignac was able to isolate this element, now recognized as Gd (III), from yttria (yttrium oxide). In 1886, the French chemist Paul Émile Lecoq de Boisbaudran confirmed Marignac's discovery, naming the new element as gadolinium, in honor to the chemist and geologist Johan Gadolin (1760-1852), who identified in a mineral, later named gadolinite, a new element showing a detectable paramagnetic resonance spectrum (Abel and Talbot 1967).

Gd (III) is found in a solid state, but never free in nature, appearing in rare-earth elements-rich minerals, such as monazite and bastnasite, besides gadolinite. It is a sensitive metal when exposed to open air, reacting with oxygen to form oxides (GdO and Gd₂O₃), and presents the following characteristics: silvery white, ductile, flexible and with a metallic glow; it is more stable in dry air, reacting slowly with water to form gadolinium hydroxide; it is soluble in strong and diluted acids, releasing hydrogen. It is also a superconductor at temperatures below 272.067 °C; it has ferromagnetism, being highly magnetic at room temperature (Haley *et al.* 1961).

Gd (III) has 6 stable isotopes - ¹⁵⁴Gd, ¹⁵⁵Gd, ¹⁵⁶Gd, ¹⁵⁷Gd, ¹⁵⁸Gd (the most abundant), ¹⁶⁰Gd, and the radioisotope ¹⁵²Gd. Gd (III) can be found in the following salt forms: chloride (GdCl₃), fluoride (GdF₃), nitride (GdN), oxide (Gd₂O₃), sulfide (Gd₂S₃), iodide (GdI₃) and bromide (GdBr₃) (Caravan *et al.* 1999). Currently, Gd (III) is obtained through ion exchange, extraction or reduction of its anhydrous fluoride with metallic calcium (Braga and Vera 2017).

Gd (III) has several applications in the industrial area (Braga and Vera 2017), namely, in the production of some electronic equipment and nuclear reactors (Elias Jr *et al.* 2008). However, the most important application of Gd (III) is due to its paramagnetic properties, that made it a crucial tool for medical diagnosis and treatment monitoring across multiple clinical settings (Perazella 2009).

Gd (III) is known to modify the resonance of protons (Caillé *et al.* 1983), improving the quality of diagnostic images; moreover, by reducing the width of the x-ray spectrum, the exposure of patients to radiation can be reduced (Burgess 1981). In magnetic resonance

imaging (MRI), Gd (III), as an ion with unpaired electrons, reduces T1 (longitudinal) and T2 (transverse) relaxation times of neighboring water protons (Elias Jr *et al.* 2008). During MR, pulses of radiofrequency are applied to the tissues in the presence of a magnetic field, inducing proton excitation inside water molecules. The energy released when protons return to their fundamental state is registered, producing an image of MR.

In the 1960s, evidence of the toxicity of Gd (III) in the salt form was reported in animal studies, showing that Gd₂O₃ caused chronic pulmonary toxicity, liver damage and could even lead to death (Ball and Van Gelder 1966). Histological analysis of lung tissues showed several injuries, namely, interstitial thickening, calcification of small pulmonary vessels, lymphoid hyperplasia, macrophage accumulation (Ball and Van Gelder 1966), alveolar cell hypertrophy and septal cell thickening (Abel and Talbot 1967).

Only in the late 1980s, the applicability of Gd (III) as a contrast agent stood out again, following the development of formulations of Gd (III) stabilized by chelating agents (de Haen 2001).

Gadolinium complexes

Contrast agents composed of chelated Gd (III), commonly referred to gadolinium-based contrast agents (GBCA), have been widely used in MRI for over 3 decades, supporting the diagnosis of tumors, pathologies of the central nervous system, lesions in blood vessels and spinal cord, sclerosis and cerebrovascular accidents (Lohrke *et al.* 2017), among other clinical disorders. Recent estimates indicate that over 450 million doses of GBCA have already been administered worldwide (Soloff and Wang 2020).

The conception of GBCA takes into account that the release of Gd (III) from chelates must be low enough to be safe. Thus, Gd (III) must attach firmly to a high affinity ligand, to form a GBCA. The main advantage of the complexed forms of Gd (III) is to reduce its toxicity, while maintaining its paramagnetic properties and increasing the sensitivity and specificity of MRI diagnostic.

The first GBCA to be synthesized and clinically evaluated was Gd (III) diethylenetriamine penta-acetic acid (*Gd-DTPA*) or *gadopentetic acid* (Carr *et al.* 1984; Runge *et al.* 1985), but several others gadolinium-chelates have been developed since then.

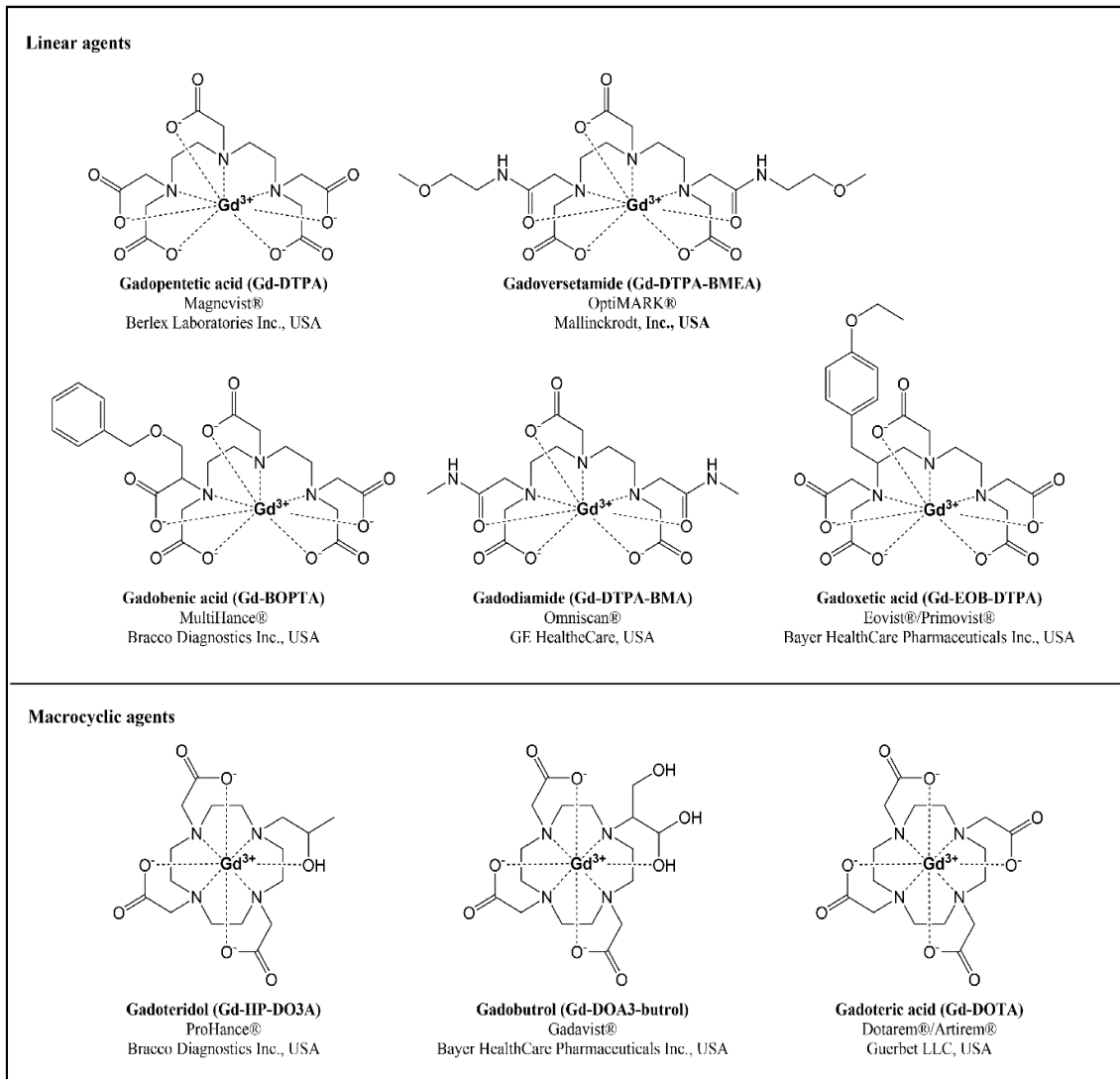


Figure 1: Chemical structures of linear and macrocyclic gadolinium-based contrast agents, brand names and registering pharmaceutical companies.

Considering the chemical structure of the chelating molecule, GBCA can be classified as linear or macrocyclic agents, if they have either an open or an enclosing structure, respectively (Figure 1). Depending on their charge, they can be ionic, like the GBCA in acidic form, or non-ionic, which includes the chelating agents with amide or alcohol groups. Linear Gd-complexes are flexible open chains that do not offer a strong bond to Gd (III), while macrocyclic GBCA, pre-arranged rigid rings of almost ideal size to trap the ion, offer a stronger connection to Gd (III). The development of macrocyclic chelates was prompted by the low stability of linear GBCA. Gd (III) dissociates more quickly and easily from linear chelates, which results in higher circulating levels and increased tissue uptake of free Gd (III), entailing long-term deleterious consequences for multiple organs (Mundim *et al.* 2009).

Due to their enclosed structure, the macrocyclic GBCA are thermodynamically more stable, losing less Gd (III) per unit of time; thus, they appear to be inert under physiological conditions (Broome *et al.* 2007). Non-ionic complexes seem to be less stable than ionic complexes, because the link of Gd (III) with negatively charged carboxyl groups is stronger, compared to non-ionic chelates with amides or alcohol. According to the stability constants and kinetic evaluations, the most stable GBCA seem to be the ionic macrocyclic GBCA, and the non-ionic linear chelates gadodiamide and gadoversetamide, the less stable agents (Abujudeh *et al.* 2010).

GBCA pharmacokinetics and Gd (III) tissue deposition

The GBCA are mainly administered intravenously (*i.v.*). The dose deemed safe for most GBCA is 0.1 mmol/Kg of body weight, with the exception of the liver specific GBCA gadoxetic acid, for which a lower dose of 0.025 mmol/Kg was approved. For MR angiography, a double or triple GBCA dose can be administered, whenever necessary, to improve imaging (Aime and Caravan 2009).

GBCA were designed to be completely excreted after their administration and subsequent distribution. After *i.v.* administration, Gd (III) chelates rapidly reach a balance between the intravascular and interstitial fluids. Depending on its structure, the complex can also gain intracellular compartments (*e.g.* liver and kidneys) by passive diffusion or by specific uptake processes (Aime and Caravan 2009). Clinically, GBCA are classified according to their distribution, as extracellular fluid agents (also called extracellular space agents), liver agents, and intravascular or blood pool agents (Aime and Caravan 2009).

Extracellular GBCA are eliminated by the kidney. In case of normal renal function, the compound is almost entirely (>90%) recovered from the urine after 12 hours, and completely recovered after 7 days, in case of normal or moderately impaired renal function. Since the rate of elimination is lower in patients with renal disease, the plasma half-life of the compound increases substantially, from hours to days, depending on the level of renal function compromise (Aime and Caravan 2009).

Liver agents (gadobenic and gadoxetic acid) can be captured by hepatocytes and cleared via the hepatobiliary system. These GBCA have dual elimination pathways, 2-4% of gadobenic acid and 50% of the gadoxetic acid, is eliminated through the hepatic pathway,

and the remainder by the kidneys. In case of renal impairment, as these GBCA have dual elimination pathways, the renal elimination might be replaced by the hepatic elimination, decreasing Gd (III) accumulation in the body (Altun *et al.* 2009). In patients with hepatic impairment, there is little impact on the pharmacokinetics of these agents (Aime and Caravan 2009).

Blood pool agents bind reversibly to serum albumin, preventing distribution into the interstitial space, staying in vascular system for a significant period (Choi and Moon 2019).

Pharmacokinetic studies showed that Gd (III) is not totally recovered in urine of patients with severe renal failure (Aime and Caravan 2009). *In vivo*, the Gd-complex is surrounded by a variety of competing molecules, which have the ability to interact with Gd (III) or with its ligand. Different endogenous cations, such as iron, magnesium, copper, zinc or calcium, compete with Gd (III) ions for the ligand, replacing it, in an organometallic dechelating reaction, known as transmetallation (Corot *et al.* 1998; Frenzel *et al.* 2008; Hao *et al.* 2012). Endogenous anions, like phosphate, carbonate, citrate and hydroxide, can then bind to free Gd (III), precipitating in different tissues (Figure 2).

Thus, free Gd (III) ion regains its toxic properties by interacting with endogenous molecules and through activation/inhibition of different biological processes (Lancelot 2016).

Accumulation of Gd (III) ion has been reported in brain (Kanda *et al.* 2014), kidney (Grobner 2006; Sato *et al.* 2013), liver (Mercantepe *et al.* 2018), skin (Do *et al.* 2014) and bone tissue (Damme *et al.* 2020). Its retention in biological tissues rises in those who have recurrent exposure to GBCA, and it appears to last for several years (Wagner *et al.* 2016). Gd (III) can be found in bone tissue up to 5 years after administration of GBCA (Lord *et al.* 2018). Animal studies showed that the amounts of Gd (III) retained in the bones, brain, skin and other organs, are higher for linear GBCA than for those with a macrocyclic structure (Choi and Moon 2019; Kanal and Tweedle 2015; Sherry *et al.* 2009). In *postmortem* cases of patients with nephrogenic systemic fibrosis (NSF), a clinical complication observed in subjects with compromised renal function after exposure to GBCA (Grobner 2006), Gd (III) was found in all analyzed tissues, showing very high levels in the kidney, heart and blood vessels (Kay *et al.* 2008). Skin biopsies of NSF patients, showed deposition of insoluble Gd (III), predominantly in the deep dermis and

subcutaneous fibrous septa (Thakral and Abraham 2009). High concentrations of Gd (III) persisted in the skin, up to 3 years after the last exposure to GBCA (Thakral *et al.* 2007). This long-term retention of Gd (III) raises concerns about the safety of GBCA, once the random subsequent mobilization of such deposits may result in a variable onset latency of adverse effects.

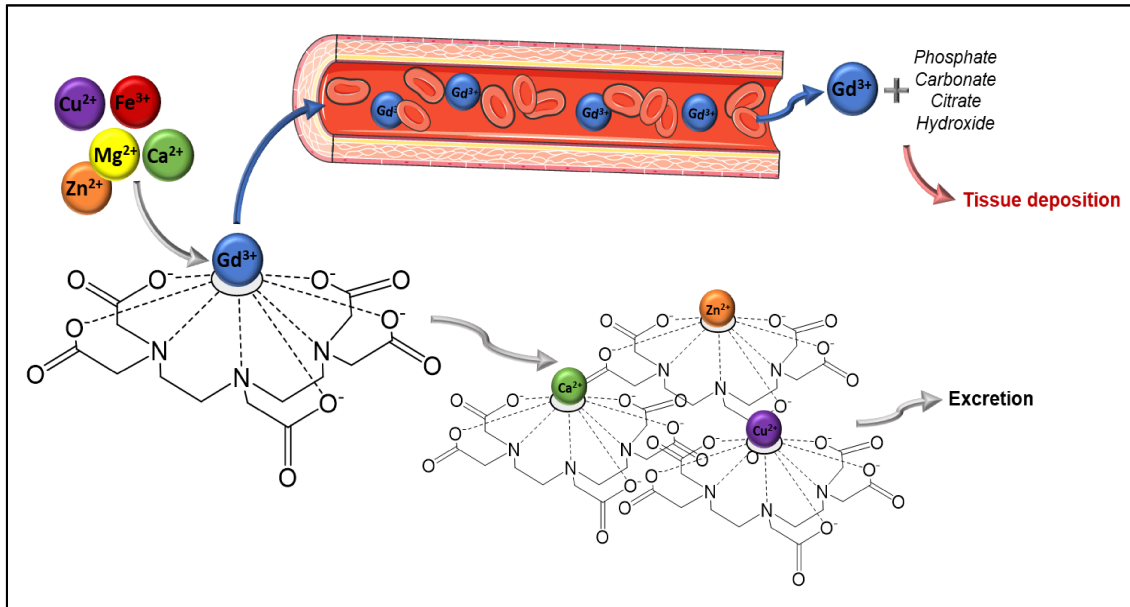


Figure 2: Process of dechelation (transmetallation) of Gd (III) from GBCA by endogenous cations. Substituted chelates are excreted from the organism. Ionic Gd (III) can precipitate in the presence of endogenous anionic molecules, and deposit in different tissues.

General adverse effects

For several years, GBCA were considered to have an optimal pharmacological profile, with reported acute adverse reaction rates ranging from 0.01 to 2% and with severe adverse reaction rates of only 0.01 to 0.04% (Bussi *et al.* 2018).

Considering the ability of GBCA to cross the placenta in pregnant women and its presence in the milk of lactating women, their use is not recommended in these situations (Elias Jr *et al.* 2008).

Adverse effects of GBCA appear to occur less frequently than for iodinated contrast agents, which were previously used in MRI exams and partially replaced by GBCA; although much safer, immediate reactions to GBCA have been reported in large case series (Granata *et al.* 2016). The acute adverse reactions to GBCA are classified according

to clinical severity, in major/severe or minor reactions, and according to their localization, in widespread and local adverse reactions (Elias Jr *et al.* 2008). Cases of acute adverse reactions, such as laryngospasm and anaphylactic shock, are rare (Li *et al.* 2006). Nonetheless, one case of a fatal anaphylactic reaction to gadobutrol, a macrocyclic GBCA, was reported (Franckenberg *et al.* 2018). Common minor reactions include nausea, vomiting, hives, and headache; skin irritation, itching, itching or cold feeling, have been also reported (Elias Jr *et al.* 2008). Considering the low rate of acute adverse reactions, GBCA are considered as safe (Abujudeh *et al.* 2010; Uhlig *et al.* 2019).

According to Behzadi *et al.* (Behzadi *et al.* 2018) there are differences in the rate of immediate allergic reactions, when comparing ionic *versus* non-ionic, linear *versus* macrocyclic and protein-binding *versus* non-protein binding GBCA. Surprisingly, gadodiamide, a non-ionic linear GBCA, was reported to have the lowest rate of immediate allergic adverse events compared to linear ionic or to non-ionic macrocyclic GBCA; a higher rate of immediate allergic adverse reactions was associated with ionicity, protein binding and macrocyclic structure of GBCA (Behzadi *et al.* 2018). On the other hand, a study done to verify acute adverse events in Gd (III)-enhanced cardiac MRI reported that patients that used gadobenate dimeglumine, gadopentetate dimeglumine (both ionic linear GBCA) and gadoteridol (non-ionic macrocyclic GBCA), compared to those receiving gadobutrol (non-ionic *macrocyclic GBCA*), were more likely to develop acute adverse effects; patients who received gadodiamide (non-ionic linear GBCA) and gadoteric acid (ionic *macrocyclic GBCA*) were less prone to adverse effects (Uhlig *et al.* 2019).

In a 58-year-old woman, recurrent acute pancreatitis was registered 3 hours after use of gadobenate dimeglumine (Blasco-Perrin *et al.* 2013).

The use of GBCA may also cause interferences in different analytical determinations, namely, in calcium, angiotensin-converting enzyme, zinc, magnesium, total iron binding capacity, iron (Proctor *et al.* 2004), bilirubin (Niendorf and Seifert 1988), creatinine (Haylor *et al.* 2009) and sodium (Otnes *et al.* 2017).

Chronic complications related with GBCA were also described, namely, NSF that is more common in patients with renal dysfunction, a rare adverse event that usually starts with dermatological manifestations, followed by the fibrotic renal complications (Grobner 2006). In patients with renal failure, since GBCA excretion is compromised, the opportunity for chelates to release Gd (III) is enhanced, favoring NSF. It seems that Gd

(III) may trigger fibrosis under favorable conditions, as renal insufficiency (Thakral and Abraham 2009). Besides, NSF may take years to manifest (Clases *et al.* 2019)

In some patients, these fibrotic changes were also observed in the lungs. Furthermore, cardiac involvement may also occur, as reported in a *postmortem* study of a renal disease patient showing fibrotic alterations in the myocardium (Grobner 2006). Other systemic effects, including arteriovenous fistula thrombosis in hemodialysis patients, peripheral vascular occlusion, transient ischemic attack, and multiple cerebral infarctions, have been also reported (Mundim *et al.* 2009).

Since the bone serves as a storage location, Gd (III) toxicity may be a consequence of its persistent and slow release from bones (Thakral *et al.* 2007).

Gadodiamide and gadoteric acid were also found to cause hepatocellular necrosis and apoptosis by causing hepatocytes damage (Mercantepe *et al.* 2018).

The type and severity of adverse effects appear to be dependent of the chemical structure and ionicity of the GBCA, and their affinity for serum proteins (McDonald *et al.* 2019).

Renal toxicity and adverse effects in renal failure

In the last decades, concerns regarding potential long-term adverse effects of GBCA have emerged. Actually, since GBCA and iodinated contrast agents have similar characteristics, namely hyperosmolar renal excretion through glomerular filtration, the concerns about their possible nephrotoxicity have already been raised. Studies in low-risk patients suggested a benign renal profile for GBCA; however, reports of NSF occurrence in patients with advanced kidney disease exposed to GBCA, reinforced the alarm on their nephrotoxicity (Clases *et al.* 2019; Grobner 2006).

NSF is a rare condition that at presentation may resemble a skin disease, like scleroderma and scleromyxedema, but may progressively worsen, affecting different organs; it occurs in patients with renal failure, particularly in those undergoing dialysis or close to end-stage renal disease (Khurana *et al.*, 2007). This progressive disease is characterized by thickening and hardening of the skin. Itching and acute pain are often reported along with skin lesions. Chronic headaches, bone and joint pain, and blurred mental acuity have been also reported in NSF patients. The progress of fibrosis may involve muscles, leading to

member contractures and decreased mobility (Kalogeromitros *et al.* 2007), liver, heart and lungs; it has been also associated with vascular and hemostatic disorders (Kanda *et al.* 2014). Patients with metabolic acidosis who underwent MR angiography may also develop this complication, suggesting that metabolic acidosis might also be a risk factor for NSF (Elias Jr *et al.* 2008). Since NSF may be clinically occult, it is likely that its prevalence may be higher than described (Othersen *et al.* 2007).

The exact pathophysiology of NSF remains unknown and appears to be independent of gender, race, or age (Kanda *et al.* 2014). The dissociation of Gd (III) from Gd-chelates that has been pointed as the primary etiology, is more likely to occur in patients with renal failure, which have a reduced excretion rate, giving extra time for *in vivo* ion dissociation, when compared to those with normal renal function. Most reported cases of NSF were associated with the administration of non-ionic linear gadodiamide, although cases with the linear ionic agent gadopentetic acid and with the non-ionic linear agent gadoversetamide were also described (Broome 2008). It seems that in patients with end-stage renal disease, an excessive exposition to Gd (III) allows its release from endothelial blood vessels, due to trauma, endothelial dysfunction or chronic edema, favoring its accumulation in different tissues. Once inside the tissues, macrophages containing Gd (III) produce pro-fibrotic cytokines that act locally and stimulate the fibrotic response (High *et al.* 2007). In patients with multiple risk factors, GBCA have been associated with nephropathy, even at doses below 0.2 mmol/kg body weight (Thomsen 2004). Diabetic nephropathy and low glomerular filtration rate were proposed as risk factors for worsening of the renal disease, often evolving to acute renal failure, after Gd (III) administration (Ergun *et al.* 2006).

Accumulation of Gd (III) in the kidney, as well in other organs, has been reported in individuals without renal dysfunction (Rogosnitzky and Branch 2016); particularly in those submitted to repeated administrations of GBCA (Rogosnitzky and Branch 2016). According to Do *et al.* (Do *et al.* 2020), GBCA turn the tubular cells more prone to Gd toxicity effects. The observation of renal damage and tissue accumulation of Gd (III) after GBCA exposure, in subjects without previous renal disease, suggests the involvement of other mechanisms, beyond the decrease in Gd (III) elimination due to impaired renal function. Clinicians should carefully assess the need of MRIs for diagnosis, both in patients with or without renal disease (Akgun *et al.* 2006), and should restrain MRIs orderings in

patients with renal dysfunction unless it reveals essential to diagnostic (McKoy *et al.* 2008).

Mechanisms of toxicity – *in vivo* and *in vitro* studies

Gd (III) released into bloodstream can precipitate in cell membranes, organs, and bone matrices, and/or react with biomolecules, resulting in toxic effects (Carr *et al.* 1984). According to Evans (Evans 1990), after dissociation from the chelate complex, Gd (III) forms complexes with endogenous molecules, such as peptides, proteins (as plasma albumin), or metalloenzymes; when the complexation capacity is exceeded, it forms colloidal precipitates that are phagocytosed by macrophages of the reticuloendothelial system (RES).

Apoptosis, oxidative stress and competition of Gd (III) with calcium, needed for cellular processes, were pointed as potential mechanisms of Gd cytotoxicity (Rogosnitzky and Branch 2016). The Gd (III) may block calcium transport in tissues with a lower excretion rate, increasing toxicity at neuronal (Abraham and Thakral 2008; Lohrke *et al.* 2017) and cardiovascular (Swaminathan *et al.* 2008) levels. It may inhibit some enzymes that are activated by calcium, interfering with the RES, as well as with other calcium-dependent biological processes (Evans 1990); it can disturb physiological processes, like contraction of smooth, skeletal, and cardiac muscles, transmission of nervous influx, and blood coagulation (Rogowska *et al.* 2018).

Cell culture studies have shown that Gd (III) may lead to abnormal calcification of several types of cultured cells (Okada *et al.* 2011). It was shown to induce calcium deposition in MC3T3-E1 cells (pre-osteoblastic cells), human adipose tissue-derived mesenchymal stem cells, and in human dermal fibroblasts in osteogenic differentiation media; moreover, although it did not increase mRNA expression of type I collagen in human dermal fibroblasts, it promoted cell proliferation (Okada *et al.* 2011). NSF may be, at least in part, a consequence of this alteration in the calcification process, which promotes hardening of the skin and fibrotic changes in other tissues and organs.

The release of chemokines by activated cells of the RES, following Gd (III) release from GBCA, triggers the mobilization of CD34⁺ fibrocytes, favoring fibrosis; this hypothesis was raised for the pathogenesis NSF (Del Galdo *et al.* 2010; Idee *et al.* 2014).

The exposure of monocytes to GBCA induced the expression of several profibrotic chemokines, cytokines, and growth factors (Wermuth and Jimenez 2014). Gadodiamide and gadopentetate seem to stimulate macrophages and monocytes to release profibrotic cytokines and growth factors capable of initiating and supporting tissue fibrosis, characteristic of NSF (Newton and Jimenez 2009). In addition, it was found that Omniscan®, Magnevist®, MultiHance® and ProHance® increased the proliferation of human dermal fibroblasts (Newton and Jimenez 2009). In an animal study, the exposure to GBCA induced a reduction in circulating leukocytes, an increase in the levels of pro-inflammatory interleukin-6 and tumor necrosis factor receptor, and hepatic histopathological changes (vacuolar degeneration, disorganized liver cords) (Chen *et al.* 2015).

High levels of reactive oxygen species (ROS) seem to be the cause of Gd (III) induction of apoptosis in hepatocytes (Liu *et al.* 2003). The oxidative stress induced by Gd (III) also triggered endoplasmic reticulum stress in rat cortical neurons (Xia *et al.* 2011).

Other possible mechanisms for Gd (III) toxicity include blockage of adenosine diphosphate and adenosine triphosphate (ATP) hydrolysis through stimulation of angiotensin II AT1 receptors (Angeli *et al.* 2011), changes in the activity of angiotensin-converting enzyme via transmetallation with zinc (Corot *et al.* 1998), and, mobilization of iron and differentiation of mononuclear cells into ferroportin-expressing fibrocytic cells (Bose *et al.* 2015).

A slower elimination of Gd (III), due to kidney dysfunction, increases the potential for Gd (III) accumulation in kidney, brain (Clases *et al.* 2019) and other tissues. As kidneys are the principal organ of choice for GBCA excretion, proximal tubular cells are the preferential target of toxicity (Bajaj *et al.* 2018). *In vitro* and animal studies revealed that exposure to GBCA induces necrosis and apoptosis in tubular cells (Heinrich *et al.* 2007); reduces glomerular filtration rate (Elmstahl *et al.* 2006); causes kidney injury and significant metabolic alterations, particularly in renal lipid metabolism (Do *et al.* 2020). A study of extravascular toxicity demonstrated that, in rats, Gd-DTPA caused moderate necrosis, hemorrhage and edema at the site of injection (Cohan *et al.* 1991). GBCA were reported to not induce fewer cytotoxic effects on cultured renal tubular cells than iomeprol, an iodinated contrast agent; besides, among the contrast agents evaluated, gadopentetate and gadobenate formulations were found to be the ones that induced more

renal necrosis and apoptosis (Heinrich *et al.* 2007). GBCA mechanisms of toxicity at target organs, including the kidney, are far from completely clarified.

Regulatory actions for GBCA use

In 2015, the Food and Drug Administration (FDA) reported an investigation on the risk of Gd (III) brain deposits, following repeated use of GBCA. In order to reduce the potential Gd (III) accumulation, FDA alerted health care professionals for this risk and recommended to limit the use of GBCA to clinical conditions needing additional information that could only be provided by these contrast agents; and, furthermore, to carefully consider the need for recurrent MRIs (FDA 2015).

In 2016, the European Medicines Agency (EMA)'s Pharmacovigilance Risk Assessment Committee (PRAC) recommended the removal of some information from the summary of product characteristics, namely those stating that intact GBCA were unable to pass the blood-brain barrier, and requested the update of the safety specifications, namely those concerning the potentially associated risk; the PRAC also stated that a European Union review on Gd (III) security was necessary (Lancelot and Desche 2020).

The possibility of Gd (III) retention in body tissues, as a consequence of its detachment from linear GBCA, led EMA to recommend a restriction in their use (Dekkers *et al.* 2018).

Later, EMA suspended its previous authorization for introduction in the Market of some linear structure contrast agents, namely, gadodiamide (Omniscan®), gadopentetic acid (Magnevist®) and gadoversetamide (Optimark®). The use of gadoxetic acid (Primovist®) and gadobenic acid (MultiHance®) was restricted to liver MRIs, as they undergo biliary excretion, meeting an important diagnostic need. Gadopentetic acid was restricted to intra-articular administration for MRIs of the joints, since the dose necessary for this exam is very low. EMA recommended the use of agents with a macrocyclic molecular structure (as gadoteric acid, gadobutrol and gadoteridol), at the lowest dose necessary for diagnosis, and only if this is not possible without the use of contrast agents (Infarmed 2017).

Although no restrictions were made for the use of macrocyclic GBCA, several human and animal studies had already demonstrated that their use leads to Gd (III) retention in body tissues (Bussi *et al.* 2020), which was also reported in patients with normal renal function (Murata *et al.* 2016). The development of NSF, following the use of macrocyclic GBCA (e.g. gadoteric acid, gadoteridol and gadobutrol), has been also reported, although data is not always consensual (Schieda *et al.* 2018). These data raise concerns, even on the safety of macrocyclic GBCA.

In summary, data currently available in literature supports the toxic potential of GBCA, targeting several organs, particularly the kidneys.

Despite the continuous effort to develop stable and inert agents, GBCA that are currently available for improving diagnosis through MRI may be far from safe. Considering the usefulness and vital nature of contrast agents, and the lack of reliable alternatives to GBCA, it appears to be vital to characterize the molecular and cellular mechanisms underlying Gd (III) cytotoxicity, as well as to identify the pharmacological effects triggered by GBCA, clarifying the influence of pre-existing renal dysfunction in these effects.

II. Aims

Given the negative impact of exposure to contrast agents containing Gd (III) on renal function, even in individuals without pre-existing renal failure, there is a clear need to further investigate the potential for toxicity resulting from such exposure. Advances in the identification of the mechanisms of Gd (III)-induced toxicity might contribute to clarify the processes of initiation of nephrotoxicity, systemic fibrosis and acute tubular necrosis, and further guide the development of possible approaches for their prevention and/or treatment.

The aim of this study was to evaluate the nephrotoxicity mechanisms of Gd (III). The renal proximal tubule is the major target of toxicity within the nephrons, since it is where most non-filtered xenobiotics are metabolized. For this reason, a human proximal tubular cell line (HK-2 cells) was selected to investigate the effects of Gd (III).

To determine the toxic potential of Gd (III), HK-2 cells were exposed to a wide concentration range of $GdCl_3 \cdot 6H_2O$, for 24 h; the concentrations eliciting 1, 10, 25 and 50 % inhibition of cell viability (ICs) were estimated through the thiazolyl blue tetrazolium bromide (MTT) reduction assay; the viability of cells was also assessed at different time-points (2 to 48 h).

In order to investigate the mechanisms involved in the nephrotoxicity of Gd (III), we studied biomarkers of oxidative stress, mitochondrial dysfunction and cell death/survival pathways, after a 24 h exposure to Gd (III), at the estimated ICs – total and oxidized glutathione (tGSH and GSSG; respectively) contents; total antioxidant status (TAS); *NRF2* mRNA expression; intracellular levels of free calcium; mitochondrial membrane potential; intracellular adenosine triphosphate (ATP) levels; *CASP3* and *SQSTM1* mRNA expression; B-cell lymphoma 2 (Bcl-2) protein expression; lactate dehydrogenase (LDH) leakage; and morphologic changes of cells' chromatin. Gd (III) effects on renal lipid metabolism were also investigated through the assessment of lipid droplets formation, *ACACA* and *CPT1A* mRNA expression and neutral red uptake.

Aiming at determining the effects of Gd (III) on different pathophysiological responses, gene and protein expression of different modulators related to inflammation, fibrosis, hypoxia, and even the circadian cycle, was evaluated by Western Blot and quantitative polymerase chain reaction (qPCR).

III. Experimental Work

Cellular and molecular pathways underlying the nephrotoxicity of gadolinium

Nícia Reis Sousa^{1,2}, Susana Rocha³, Alice Santos-Silva^{4,5}, Susana Coimbra^{1,4,5,*}, Maria João Valente^{4,5}*

¹TOXRUN – Toxicology Research Unit, University Institute of Health Sciences, CESPU, CRL, Gandra, Portugal

²Departamento de Ciências e Tecnologia da Saúde, Instituto Superior Politécnico de Benguela, Benguela, Angola

³LAQV, REQUIMTE, Laboratório de Química Aplicada, Departamento de Ciências Químicas, Faculdade de Farmácia da Universidade do Porto, Porto, Portugal

⁴Associate Laboratory i4HB - Institute for Health and Bioeconomy, Faculdade de Farmácia da Universidade do Porto, Porto, Portugal

⁵UCIBIO – Applied Molecular Biosciences Unit, Department of Biological Sciences, Faculdade de Farmácia da Universidade do Porto, Porto, Portugal

*Corresponding authors:

e-mail addresses:

assilva@ff.up.pt (A. Santos-Silva); ssn.coimbra@gmail.com (S. Coimbra)

Keywords

Gadolinium; nephrotoxicity; oxidative stress; mitochondrial dysfunction; lipid metabolism; inflammation

Running head: *In vitro* nephrotoxic mechanisms of gadolinium

Abstract

Mounting evidence on the short- and long-term adverse effects associated with gadolinium [Gd (III)]-based contrast agents used in magnetic resonance imaging have emerged in the past three decades. Safety issues arise from the release of Gd (III) from chelates and its deposition in tissues, which is exacerbated in patients with renal disease, since the kidney is the major excretion organ of most of these agents. This study aimed at unveiling the cellular and molecular mechanisms of nephrotoxicity of Gd (III), using an *in vitro* model of human proximal tubular cells (HK-2 cell line). Cell viability declined in a concentration- and time-dependent manner after exposure to $\text{GdCl}_3 \cdot 6\text{H}_2\text{O}$. The estimated inhibitory concentrations (ICs) eliciting 1 to 50 % of cell death, after 24 h of exposure, ranged from 3.4 to 340.5 μM . At toxic concentrations, exposure to Gd (III) led to disruption of the oxidative status, mitochondrial dysfunction, cell death by apoptosis, switching to necrosis at higher levels, and autophagic activation. Disturbance of the lipid metabolism was already observed at low-toxicity ICs, with accumulation of lipid droplets, and upregulation of genes related to both lipogenesis and lipolysis. Gd (III)-exposure, even at the subtoxic IC_{01} , increased the expression of modulators of various signaling pathways involved in the development and progression of renal disease, including inflammation, hypoxia and fibrosis. Our results give new insights into the mechanisms underlying the nephrotoxic potential of Gd (III) and highlight the need to further clarify the risks *versus* benefits of the Gd (III)-based contrast agents currently in use.

Introduction

Gadolinium [Gd (III)]-based contrast agents (GBCA) have been used for over three decades to improve the sensitivity and specificity of magnetic resonance imaging (MRI) for numerous diagnostic indications, including infection and malignancy (Eggleston and Panizzi 2014; Zhou and Lu 2013).

For several years, GBCA were considered safe alternatives to iodinated agents, and it was believed that they were excreted from the human body mostly intact (Ledneva et al. 2009). However, recent data indicate that Gd (III) is able to easily detach from linear chelates through transmetallation by endogenous ions, and bind to hydrophobic macromolecules, or precipitate and deposit in body tissues (Garcia et al. 2017; Le Fur and

Caravan 2019). This led the European Medicines Agency to apply restrictions on the use of linear GBCA by mid-2017 (Dekkers et al. 2018). So far, no limitations were placed regarding GBCA composed by highly stable macrocyclic chelates. However, studies revealed that macrocyclic GBCA are also associated with Gd (III) retention in the brain and other tissues (Bussi et al. 2020; Murata et al. 2016).

Since renal excretion is the main elimination route for most GBCA, renal function impairment seems to enhance tissue retention of dissociated Gd (III), which favors toxicity and the occurrence of nephrogenic systemic fibrosis (NSF) (Grobner 2006), although it may take years to have clinical expression (Clases et al. 2019). Bioaccumulation of Gd (III) is also exacerbated in those who undergo recurrent exposure to GBCA (Clases et al. 2019; Wagner et al. 2016). Several studies reported Gd (III) deposition in the kidney, brain, liver, spleen, skin, muscle and bone tissue (Damme et al. 2020; Do et al. 2014; Do et al. 2020; Kanda et al. 2014; Mercantepe et al. 2018), even in the absence of renal disease (Wagner et al. 2016).

Despite the observations made regarding Gd (III) deposition following GBCA administration, data on the mechanisms of cytotoxicity of this metal, particularly in the kidney, are relatively scarce. *In vitro* and *in vivo* studies have begun uncovering the nephrotoxic effects of GBCA, which appear to include the ability to decrease the glomerular filtration rate (Elmstahl et al. 2006), to trigger apoptotic and necrotic cell death in proximal tubular cells (Heinrich et al. 2007), to promote renal fibrosis, and to induce metabolic dysfunction, with particular impact on the renal lipid metabolism (Do et al. 2019).

Understanding the pathways involved in the nephrotoxicity of Gd (III) can help determine the clinical significance of its retention in the kidney, allowing a more accurate assessment of the risks associated with GBCA use.

This study aimed at evaluating the nephrotoxicity mechanisms of Gd (III). Since the renal proximal tubule is where most non-filtered xenobiotics are metabolized, it is also the major target of toxicity within the nephron. For this reason, a human proximal tubular cell line (HK-2 cells) was selected to investigate the mechanisms of oxidative stress, mitochondrial dysfunction and cell death elicited by Gd (III), as well as its effects on renal lipid metabolism and multiple pathophysiological responses.

Materials and methods

Reagents

GdCl₃.6H₂O, Dulbecco's Modified Eagle's Medium/Ham's Nutrient Mixture F12 (DMEM/F12 medium), heat-inactivated fetal bovine serum (FBS), antibiotic mixture of penicillin/streptomycin (10.000 U/mL / 10.000 µg/mL), trypsin-ethylenediaminetetraacetic acid (EDTA) solution, thiazolyl blue tetrazolium bromide (MTT), neutral red dye, 2-vinylpyridine, L-glutathione reduced (GSH) and L-glutathione oxidized disodium salt (GSSG), 5,5'-dithiobis(2-nitrobenzoic acid) (DTNB), β-nicotinamide adenine dinucleotide 2'-phosphate reduced tetrasodium salt hydrate (β-NADPH), adenosine triphosphate (ATP), luciferase from *Photinus pyralis* and D-luciferin sodium salt, bisBenzimide H 33342 trihydrochloride (Hoechst 33342), propidium iodide (PI), tetramethylrhodamine ethyl ester perchlorate (TMRE), 2,3,5-triphenyltetrazolium chloride (TPTZ), 4-amino-3-hydrazino-5-mercapto-1,2,4-triazole (Purpald), cOmplete™ mini protease inhibitor cocktail, TRI Reagent® solution, and other common chemicals of analytical grade were obtained from Sigma-Aldrich (Merck KGaA, Darmstadt, Germany). Fluo-3 AM probe and BODIPY™ 493/503 dye were obtained from Thermo Fisher Scientific (Massachusetts, EUA). CytoTox 96® non-radioactive cytotoxicity assay was purchased from Promega (Wisconsin, USA). Xpert cDNA synthesis kit and Xpert Fast SYBR 2X mastermix were purchased from GRiSP (Porto, Portugal). Custom DNA oligonucleotides were synthesized and quantified by Thermo Fisher Scientific (Massachusetts, EUA) or Frilabo (Porto, Portugal). Antibodies for Western Blot analysis were obtained from Santa Cruz Biotechnology (Texas, USA), Abcam Plc (Cambridge, UK), or Sigma-Aldrich (Merck KGaA, Darmstadt, Germany).

HK-2 cell line: routine maintenance protocol

The HK-2 cell line, obtained from the American Type Culture Collection (ATCC®, VA, USA), was selected to evaluate the renal cytotoxic mechanisms of Gd (III). HK-2 is a human immortalized cell line that retains morphologic and functional characteristics of normal adult proximal tubular epithelium (Ryan et al. 1994), which has been extensively

used to evaluate contrast media-induced acute kidney injury (Lei et al. 2018; Liu et al. 2017b; Peng et al. 2015; Zhang et al. 2018).

Cells were grown in DMEM/F12 medium, supplemented with 10 % FBS, 100 U/mL penicillin and 100 µg/mL streptomycin, and maintained in a humidified incubator, at 37°C, under a 5 % CO₂ atmosphere. Cells were split, upon reaching approximately 80 % of confluency, through cell detachment by trypsinization. All assays were performed within 10 subcultures, from passages 15 to 24, to avoid significant phenotypic and functional deviations between independent experiments.

Cell plating and exposure to Gd (III)

Cells were cultured at a density of 50 000 cells/cm² and allowed to attach overnight prior to exposure. For the estimation of the inhibitory concentrations (ICs), cells were exposed to GdCl₃.6H₂O, prepared in serum-free medium, for 24 h at 37 °C, in a range of concentrations that covered non-toxic to worst-case approach effect (500 nM - 100 mM), as determined by MTT reduction assay, an indirect measure of cell viability. The estimated ICs eliciting 1, 10, 25 and 50% of viability loss (IC₀₁, IC₁₀, IC₂₅ and IC₅₀, respectively) were further used for the assessment of the mechanisms of cytotoxicity triggered by Gd (III) in HK-2 cells. All exposures were conducted in serum-free medium to avoid potential binding of Gd (III) to serum components, which could lead to undervaluation of effects. Control conditions were equally prepared in serum-free medium. At least five independent experiments were performed for all assays.

Cell viability assays

Cell viability was evaluated after exposure to GdCl₃.6H₂O through three indirect measurements: MTT reduction, lactate dehydrogenase (LDH) leakage and neutral red uptake assays. For the MTT reduction assay (Valente et al. 2012), exposed cells were incubated with 0.5 mg/mL MTT for 60 min, at 37 °C, the formed formazan crystals were dissolved in DMSO and the absorbance of the solution read at 550 nm in plate reader (PowerWaveX, Bio-Tek, Winooski, VT, USA). LDH release was quantified using the CytoTox 96® Non-Radioactive Cytotoxicity Assay (Promega, Wisconsin, USA), according to the manufacture's protocol. For this assay, the incubation medium of each

well was transferred into a new 96-well plate, and samples were incubated, at room temperature, with an equal volume of CytoTox 96® reagent. After 30 min, stop solution was added to each well, and the absorbance was recorded at 490 nm in a plate reader (PowerWaveX, Bio-Tek, Winooski, VT, USA). For evaluation of the lysosomal uptake of neutral red (Dias da Silva et al. 2019), exposed cells were incubated with a 50 µg/mL neutral red dye for 90 min, at 37 °C, washed with phosphate-buffered saline (PBS), and lysed (lysis solution: 50 % ethanol, 1 % glacial acetic acid) for further detection of retained dye at 540 nm, in a plate reader (PowerWaveX, Bio-Tek, Winooski, VT, USA). All results were normalized to a negative (cells exposed to serum-free medium) and a positive (cells treated with 1% Triton X-100) control, which are represented as dashed horizontal lines.

Intracellular levels of GSH and GSSG

Total and oxidized glutathione (tGSH and GSSG, respectively) contents were determined using the DTNB-GSSG reductase recycling assay (Dias da Silva et al. 2019). Briefly, cells exposed in 6-well plates were collected and precipitated with 5 % perchloric acid, centrifuged at 11,000g, for 5 min, at 4°C, and the supernatant was then neutralized with 0.76 M KHCO₃. Neutralized samples were centrifuged (11 000g, 1 min). Reagent solution (0.24 mM β-NADPH and 0.7 mM DTNB in 71.5 mM phosphate buffer with 0.63 mM EDTA, final concentration in wells) was added to the supernatants and incubated for 15 min at 30 °C. A solution of 2 U/mL glutathione reductase (final concentration in wells) was then added to all samples to initiate the formation of 5-thio-2-nitrobenzoic acid, which was monitored for 3 min at 415 nm, in a plate reader (PowerWaveX, Bio-Tek, Winooski, VT, USA). For GSSG quantification, precipitated samples were incubated, prior to neutralization, with 2-vinylpyridine for 1 h, at 4 °C, with continuous agitation, allowing GSH derivatization. GSSG was then quantified as described for tGSH. Results were normalized to total protein content, as assessed by the Bradford's method. GSH levels were estimated as follows: $GSH = tGSH - (2 \times GSSG)$, and data was presented as % of control, which is represented as a dashed horizontal line.

Total antioxidant status

Total antioxidant status (TAS) of the cells was determined through the ferric reducing ability of plasma assay, adapted from Benzie and Strain (1996), a colorimetric assay based on the reduction of Fe (III) to Fe (II) under low pH. For this purpose, cell homogenates, obtained after lysis of GdCl₃·6H₂O-exposed cells (lysis buffer: 20 mM Tris-HCl, 150 mM NaCl, 5 mM EDTA, 0.3 % Triton X-100, with protease inhibitor cocktail; pH 7.5), were incubated with a 1.5-0.75 mM Fe (III)-TPTZ solution [prepared in acetate buffer (300 mM; pH = 3.6)] at 37 °C. The absorbance was read in a plate reader (PowerWaveX, Bio-Tek, Winooski, VT, USA) at 593 nm after 4 min incubation at 37°C, and the levels of Fe (II) were estimated by interpolation from a standard Fe (II) curve. Data were normalized to total protein content assessed by the Bradford's method.

Mitochondrial membrane potential

The TMRE dye was used to assess the effects of Gd (III) on the mitochondrial membrane potential ($\Delta\Psi_m$) through flow cytometry, as previously described (Crowley et al. 2016), with minor modifications. Briefly, exposed cells were collected after trypsinization, and incubated with 500 nM TMRE for 15 min, at 37 °C. Samples were then rinsed twice (300g, 4 min), resuspended in PBS and analyzed in a BD Accuri™ C6 flow cytometer (BD Biosciences, CA, USA). TMRE is a cell permeant, positively charged dye, sequestered by viable mitochondria according to the $\Delta\Psi_m$. The orange fluorescence of the probe was detected in a 585/40 nm filter (FL2 detector). 20 000 events were analyzed per sample. Data were normalized to control cells (exposed to serum-free medium), which is represented as a dashed horizontal line.

Intracellular free calcium

Calcium-binding Fluo3 fluorochrome was used to determine the intracellular levels of free calcium. For this assay, exposed cells were collected through trypsinization and centrifuged (300g, 4 min, at 4°C). The supernatant was then discarded, and cells were incubated at 37°C with 10 μ M Fluo3-AM solution prepared in serum-free DMEM-F12 medium without phenol red. After 30 min, cells were washed and resuspended with medium, and analyzed in a BD Accuri™ C6 flow cytometer (BD Biosciences, CA, USA).

The green fluorescence of Fluo3 was detected in a 533/30 nm filter (FL1 detector). The orange/red fluorescence of non-viable cells (stained with 50 μ M PI) was excluded from the analysis. 20 000 viable cells were analyzed per sample. Results were normalized to control cells (exposed to serum-free medium), which is represented as a dashed horizontal line.

Intracellular ATP levels

The ATP bioluminescence assay, based on the reaction of ATP and luciferin, catalyzed by luciferase, was performed as previously described (Dias da Silva et al. 2019), using samples collected as protocolled above for the measurement of tGSH and GSSG. Briefly, supernatants of neutralized samples were added to 96-well opaque plates and incubated with luciferin-luciferase assay solution [final concentrations: 0.15 mM luciferin, 30,000 light units of luciferase, 50 mM glycine, 10 mM MgSO₄, 1 mM Tris, 0.55 mM EDTA, 1% bovine serum albumin (pH 7.6)]. Results were normalized to total protein, measured by the Bradford's method.

Hoechst 33342/propidium iodide double staining

Cell death mechanisms were identified based on DNA probing and chromatin morphology, using Hoechst 33342, a blue-fluorescent cell-permeant nuclear DNA counterstain, and PI, a red-fluorescent membrane impermeant nuclear dye that stains non-viable cells (Valente et al. 2012). For this purpose, cells were incubated with 50 μ M PI for 10 min, at 37 °C, rinsed twice and incubated with a 10 μ g/mL Hoechst 33342 solution for 5 min, at 37 °C. The plate was then observed under an inverted fluorescent microscope (Nikon Eclipse Ti, Nikon, Amsterdam, The Netherlands), at an original magnification of 200 \times .

Fluorescent dyeing of neutral lipid droplets

The presence of cytoplasmic vesicles containing neutral lipids was assessed using the lipophilic, green fluorescent probe BODIPY™ 493/503 as previously described (Qiu and Simon 2016), with minor modifications. Briefly, cells were washed with PBS after

exposure to $GdCl_3 \cdot 6H_2O$, and incubated for 20 min, at 37 °C, with a 2 μ M solution of BODIPY™ 493/503 prepared in PBS. Cells were then rinsed twice with PBS and incubated with a 10 μ g/mL Hoechst 33342 solution for 5 min, at 37 °C. The plate was then observed under an inverted fluorescent microscope (Nikon Eclipse Ti, Nikon, Amsterdam, The Netherlands), at an original magnification of 200 \times .

Gene expression analysis

After exposure to Gd (III), cells were collected in cold TRI Reagent® solution for RNA extraction. Briefly, samples were submitted to liquid extraction with chloroform, centrifuged at 12 000g, for 15 min at 4 °C, and the RNA was then precipitated from the aqueous phase with isopropanol. After centrifugation (12 000g, for 10 min at 4 °C), the RNA-rich pellet was resuspended in 75 % ethanol, washed (7 500g, for 5 min at 4 °C) and dissolved in RNase free water, for 10 min at 58 °C. Samples were quantified using a NanoDrop™ 1000 Spectrophotometer (Thermo Fisher Scientific, Massachusetts, EUA). One microgram of total RNA was reversely transcribed using the Xpert cDNA synthesis kit (GRiSP, Porto, Portugal), following the manufacturer's instructions. Custom primer pairs (**Table 1**) and six nanograms of cDNA were used in qPCR reactions for gene expression analysis using the Xpert Fast SYBR 2X mastermix (GRiSP, Porto, Portugal) in a StepOnePlus™ Real-Time PCR System (Thermo Fisher Scientific, Massachusetts, EUA). Relative quantification of gene expression was determined using the $2^{-\Delta\Delta CT}$ method (Livak and Schmittgen 2001), using the genes encoding for beta-actin (*ACTB*) or tubulin alpha-1B chain (*TUBA1B*) for normalization.

Protein expression analysis

Gd (III) effects on the expression of different proteins were detected through Western Blotting. After exposure, cells were rinsed, incubated with cold lysis buffer (20 mM Tris HCl; 150 mM NaCl; 0.3% Triton X-100; 5 mM EDTA; pH 7.5; with protease inhibitor cocktail), for 30 min at 4 °C, and collected into tubes. Samples were then vortexed, sonicated and centrifuged (13 000g, 10 min). The supernatants were collected into new tubes and stored until assayed. Total protein content was determined through the Bradford's method. Samples containing a total of 70 – 100 μ g of total protein were

separated by reducing 9 % acrylamide/bis-acrylamide SDS-PAGE to evaluate the expression of nuclear factor-kappa B (NFκB)-p65 and brain and muscle aryl hydrocarbon receptor nuclear translocator-like protein 1 (Bmal1), while a 15 % SDS-PAGE was used for the assessment of B-cell lymphoma 2 (Bcl-2) expression.

Table 1: List of primer sequences, annealing temperatures and final concentration.

Gene	Primer sequences (5' → 3')	T_a (°C)	Concentration (nM)
<i>NRF2</i>	F GCCCCTGTTGATTTAGACGG	56	200
	R TGTCAGTTTGGCTTCTGGAC		
<i>CASP3</i>	F TAGATGGTTTGAGCCTGAGC	60	400
	R GCTTCACTTTCTTACTTGGCG		
<i>ACACA</i>	F CATGTTAAGGCGCTGGTTTG	61	400
	R CGGATTTGCTTGAGGACGTA		
<i>CPT1A</i>	F AACTCACATTCAGGCAGCAA	62	100
	R GTCTCTCATGTGCTGGATGG		
<i>SQSTM1</i>	F GGAGTCGGATAACTGTTC	58	400
	R GATTCTGGCATCTGTAGG		
<i>NFKB1</i>	F TGGTGGGAAAACACTGTGAG	60	400
	R ATAGCCCCTTATACACGCCT		
<i>IL6</i>	F GGAGACTTGCCTGGTGAAAA	55	400
	R GTCAGGGGTGGTTATTGCAT		
<i>IL1B</i>	F CATTGCTCAAGTGTCTGAAGC	57	400
	R CGGAGATTCGTAGCTGGATG		
<i>TGFβ1</i>	F CTCGCCAGAGTGGTTATCTT	60	400
	R GGTAGTGAACCCGTTGATGTC		
<i>OPN</i>	F GCCACAAGCAGTCCAGATTA	57	400
	R TTTTGGGGTCTACAACCAGC		
<i>HIF1A</i>	F CCCTAACTAGCCGAGGAAGA	61	400
	R CACAAATCAGCACCAAGCAG		
<i>ACTB</i>	F TGCCATCCTAAAAGCCACCC	56	100
	R AGACCAAAGCCTTCATACATCTC		
<i>TUBA1B</i>	F CTGGAGCACTCTGATTGT	57	200
	R ATAAGGCGGTTAAGGTTA		

F: forward; R: reverse; *NRF2*: nuclear factor erythroid-2-related factor 2; *CASP3*: caspase 3; *ACACA*: acetyl-CoA carboxylase 1; *CPT1A*: carnitine palmitoyltransferase 1A; *SQSTM1*: sequestosome-1; *NFKB1*: nuclear factor-kappa B subunit 1; *IL6*: interleukin-6; *IL1B*: interleukin-1 beta; *TGFβ1*: transforming growth factor beta 1; *OPN*: osteopontin; *HIF1A*: hypoxia-inducible factor-1 alpha; *ACTB*: beta-actin; *TUBA1B*: tubulin alpha-1B chain.

Proteins were then transferred onto nitrocellulose membranes. Immunodetection was performed after an overnight incubation with the mouse monoclonal anti-Bcl-2 (1:50), goat polyclonal anti-NFκB-p65 (1:50) or rabbit polyclonal anti-Bmal1 (1:200), followed

by a 2-hour incubation with the secondary rabbit anti-mouse (1:2000), donkey anti-goat (1:500) or goat anti-rabbit HRP conjugate antibody (1:1000), respectively. β -Actin was detected as a protein loading control, using a primary mouse monoclonal anti- β -actin antibody (1:5000) and a secondary rabbit anti-mouse HRP conjugate antibody (1:2000). Immunoreactive bands were visualized using the chemiluminescent WesternBright ECL HRP substrate, Advansta (San Jose, CA, USA) and the ChemiDoc™ Touch Imaging System (Bio-Rad, Hercules, CA, USA) and were analyzed with the Image Lab™ Software (Bio-Rad, Hercules, CA, USA). All results were normalized to a negative control (cells exposed to serum-free medium) set as 1, which is represented as a dashed horizontal line.

Statistical analysis

The complete curve of cell death, as determined by the MTT reduction assay, was fitted to the logistic regression model for normalised response (equation: $Y = \frac{100}{1+10^{X-\log(IC_{50})}}$), which was chosen based on the principles of predictive power and goodness-of-fit. The ICs eliciting 1, 10, 25 and 50% of viability loss (IC₀₁, IC₁₀, IC₂₅ and IC₅₀, respectively) were estimated from the applied regression model, with a 95 % confidence interval. Further data are presented as mean \pm standard error of the mean (SEM). Statistical analysis was performed using the GraphPad Prism 8 (version 8.0.2) for Windows. Normality of data distribution was assessed by the Shapiro-Wilk test. Multiple comparisons for parametric data were assessed by one-way ANOVA analysis, followed by Fisher's LSD post-hoc test, whereas nonparametric data were analyzed through the Kruskal-Wallis test, followed by Dunn's test. Significance was accepted for $p < 0.05$.

Results

Gd (III) induces loss of cell viability in a concentration- and time-dependent manner

We started by investigating the nephrotoxic potential of Gd (III), in the form of trichloride hexahydrate (GdCl₃·6H₂O) prepared in serum-free medium, in a wide range of concentrations, comprising no-effect to worst-case approach concentrations. In **Fig. 1a** is represented the complete concentration-response curve of the HK-2 cells exposed to 500

nM - 100 mM Gd (III) for 24 h, assessed through the MTT reduction. Reduction of water-soluble tetrazolium salts, such as MTT, is commonly attributed to mitochondrial enzymes, though it is known that this reaction may also be catalysed by other nonmitochondrial enzymes (Bernas and Dobrucki 2002). Nevertheless, this method allows an indirect assessment of cell death, based on the amount of functional cells that are able to reduce the MTT into a formazan. We observed that the exposure of HK-2 cells leads to a loss of viability in a concentration and time dependent manner. The concentrations that induce 1, 10, 25 and 50 % inhibition of cell viability (ICs) were estimated from the obtained curve (table embed in **Fig. 1a**) and were found to be at the micromolar levels (3.4 – 340.5 μ M). When exposing cells at the IC₂₅ Gd (III) at different time-points, no significant effects were observed from 2 to 8 h of exposure (**Fig. 1b**). A time-dependent loss of viability was observed from 24 to 48 h of exposure, with cell death increasing from 25 to approximately 40 % at the longest time-point tested ($p < 0.0001$ vs. control and vs. 24 h). The four estimated ICs were selected for further evaluation of the mechanisms involved in the observed nephrotoxicity.

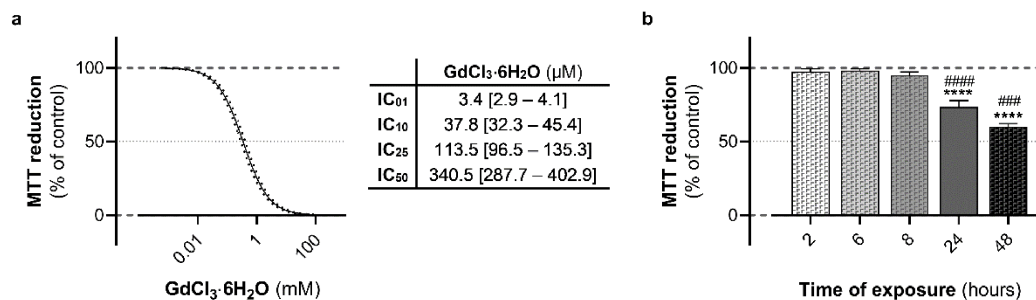


Fig. 1 (a) Nonlinear regression model for Gd (III)-induced cell death, assessed by the MTT reduction assay, in HK-2 cells exposed to 500 nM – 100 mM GdCl₃·6H₂O, for 24 h, at 37 °C. Dotted lines represent the 95 % confidence band for data obtained from 6 independent experiments performed in triplicate. Embed table: ICs [lower limit – upper limit] estimated with a 95 % confidence interval. **(b)** Effect of Gd (III) on MTT reduction in HK-2 cells exposed to IC₂₅ for 2, 6, 8, 24 or 48 h, at 37 °C. Data are presented as mean \pm SEM of 6 independent experiments, performed in triplicate. **** $p < 0.0001$ vs. control; #### $p < 0.0001$ vs. previous time-point. MTT: thiazolyl blue tetrazolium bromide; ICs: inhibitory concentrations.

Gd (III) disrupts the intracellular oxidative status

As depicted in **Fig. 2a**, Gd (III) induces a significant and identical decline in the intracellular TAS at the two highest ICs tested, dropping from 7.9 ± 0.7 in control to $6.1 \pm 0.5/0.4$ nmol Fe²⁺/mg protein at IC₂₅/IC₅₀ ($p < 0.05$ vs. control). Accordingly, Gd (III)

interfered with glutathione redox cycling (**Fig. 2b**), inducing a significant depletion of the main non-enzymatic cellular antioxidant defence, GSH, of about 31 % for the IC₂₅ ($p < 0.001$ vs. control; $p < 0.05$ vs. IC₁₀) and 57 % for the IC₅₀ ($p < 0.0001$ vs. control; $p < 0.01$ vs. IC₂₅). This effect was accompanied by a significant increase in levels of the oxidized form GSSG, starting from the IC₁₀ with an increment of 65 % ($p < 0.05$), 88 % for the IC₂₅ ($p < 0.01$), and 105 % for the IC₅₀ ($p < 0.01$) over control. As a major regulator of GSH homeostasis (Harvey et al. 2009; Steele et al. 2013), we analysed the expression of the gene encoding for the nuclear factor erythroid-2-related factor 2 (Nrf2) (**Fig. 2c**). *NRF2* was upregulated in a concentration-dependent manner, though differences from control (1.0 ± 0.1) were only significant at the IC₅₀ (2.1 ± 0.4 , $p < 0.01$).

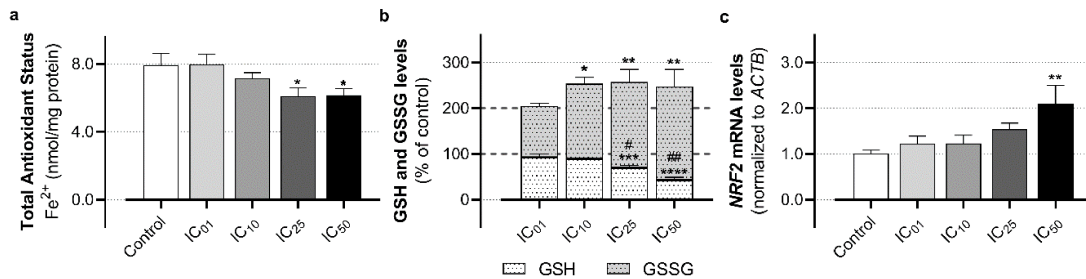


Fig. 2 Effect of Gd (III) on (a) total antioxidant status, (b) GSH and GSSG levels, and (c) *NRF2* mRNA levels, in HK-2 cells exposed to different ICs of GdCl₃·6H₂O, for 24 h, at 37 °C. Data are presented as mean ± SEM of at least 5 independent experiments, performed in duplicate or triplicate. * $p < 0.05$, ** $p < 0.01$, *** $p < 0.001$, **** $p < 0.0001$ vs. control; # $p < 0.05$, ## $p < 0.01$ vs. previous IC. IC: inhibitory concentration; GSH: reduced glutathione; GSSG: oxidized glutathione; *NRF2*: nuclear factor erythroid-2-related factor 2.

Gd (III) induces mitochondrial dysfunction

Oxidative phosphorylation at the inner mitochondrial membrane is an important source of energy for cells, and it is driven by the mitochondrial uptake of cytoplasmic Ca²⁺, which is $\Delta\Psi_m$ -dependent (Brookes et al. 2004). Since oxidative stress is closely linked to mitochondrial damage, in order to assess the impact of Gd (III) on mitochondrial function, we evaluated the $\Delta\Psi_m$, and the intracellular levels of Ca²⁺ and ATP in GdCl₃·6H₂O-exposed HK-2 cells (**Fig. 3**). It was possible to observe a rise in Ca²⁺ levels along with the increase in Gd (III) concentration (**Fig. 3a**). However, this effect was only significantly different from control ($3.0 \pm 0.6 \times 10^5$ RFU) for the two highest ICs, presenting an increase in Fluo3-AM green fluorescence of $5.3 \pm 0.6 \times 10^5$ RFU ($p < 0.05$) for IC₂₅ and $7.3 \pm 0.7 \times 10^5$ RFU ($p < 0.001$) for IC₅₀. Depolarization of the mitochondrial

membrane was also observed at the IC₅₀ (**Fig. 3b**), with a decrease in TMRE fluorescence of about 38 % below control ($p < 0.01$). Gd (III) also induced a depletion of the intracellular levels of ATP (**Fig. 3c**) of approximately 25 % for the IC₂₅ ($p < 0.001$ vs. control) and of 52 % for the IC₅₀. ($p < 0.0001$ vs. control), confirming a disturbance of the cells' energetic homeostasis.

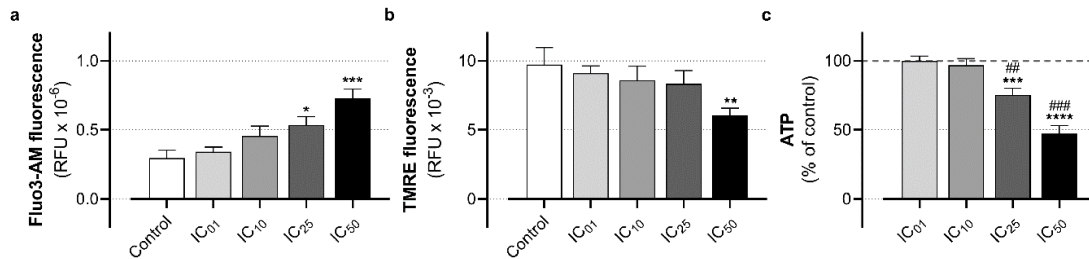


Fig. 3 Effect of Gd (III) on (a) intracellular calcium, (b) mitochondrial uptake of TMRE, and (c) ATP levels in HK-2 cells exposed to different ICs of GdCl₃·6H₂O, for 24 h, at 37 °C. Data are presented as mean ± SEM of at least 5 independent experiments. * $p < 0.05$, ** $p < 0.01$, *** $p < 0.001$, **** $p < 0.0001$ vs. control; ## $p < 0.01$, ### $p < 0.001$ vs. previous IC. IC: inhibitory concentration; TMRE: tetramethylrhodamine ethyl ester perchlorate; ATP: adenosine triphosphate.

Gd (III) activates programmed and non-programmed cell death

Following mitochondrial damage, and specifically Ca²⁺ overload and $\Delta\Psi_m$ disruption, the pro-apoptotic signaling pathway is initiated (Ly et al. 2003). Apoptosis is an energy-dependent mechanism and thus, with the progression of damage and subsequent ATP exhaustion, a switch to necrotic cell death may occur (Eguchi et al. 1997). In line with this, exposure of cells to Gd (III) resulted in cell death, characterized by morphological changes from control cells (**Fig. 4a**) consistent with apoptosis at lower concentrations of Gd (III). Condensed nuclei stained with Hoechst 33342 were already observed at the IC₀₁ (**Fig. 4b**; green arrows – early apoptotic nuclei) and double stained condensed nuclei at the IC₁₀ (**Fig. 4c**; orange arrow – late apoptotic nuclei); apoptotic cells were also observed at the highest concentrations. Necrotic cells, which appear with double stained non-condensed chromatin, were observed at the IC₂₅ (**Fig. 4d**; red arrow – necrotic nuclei), though higher prevalence of necrosis was observed at the IC₅₀ (**Fig. 4e**).

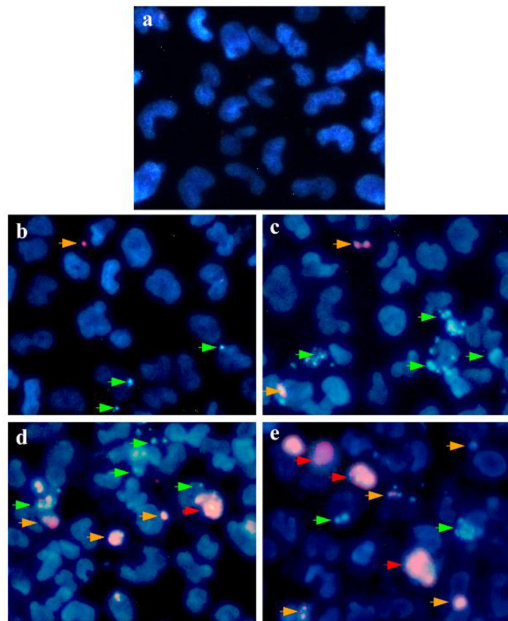


Fig. 4 Representative fluorescence microscopy images of Hoechst 33342/PI double staining of (a) control HK-2 cells, and cells exposed to (b) IC₀₁, (c) IC₁₀, (d) IC₂₅ and (e) IC₅₀ GdCl₃·6H₂O, for 24 h, at 37°C. Green, yellow and red arrows indicate early apoptotic, late apoptotic, and necrotic nuclei, respectively. Original magnification of 200×. IC: inhibitory concentration.

As shown in **Fig. 5a**, at the two highest concentrations tested, Gd (III) induced an upregulation of *CASP3* of approximately 1.5-fold over control ($p < 0.01$). A significant decrease of about 23 % in the expression of the protein Bcl-2 was also found from IC₁₀ onwards (**Fig. 5b**; $p < 0.05$ vs. control).

LDH release was assessed as a marker of cell membrane integrity and, therefore, of necrosis. Compared to control, it was also observed an increase in extracellular LDH of 19.0 ± 8.4 ($p < 0.01$) and 26.8 ± 7.7 % ($p < 0.001$) for the IC₂₅ and IC₅₀, respectively (**Fig. 5c**).

Besides inhibiting apoptosis, Bcl-2 protein is also a key modulator of autophagy (Levine et al. 2008). For this reason, we also evaluated the expression of *SQSM1*, the gene encoding for the autophagy receptor sequestosome-1, or p62, and found an upregulation in Gd (III)-exposed cells when compared to control (1.0 ± 0.1), which was significant from IC₁₀ onwards, with an expression of 1.5 ± 0.1 , 1.9 ± 0.2 and 2.2 ± 0.2 for IC₁₀ ($p < 0.05$), IC₂₅ ($p < 0.001$) and IC₅₀ ($p < 0.0001$), respectively (**Fig. 5d**).

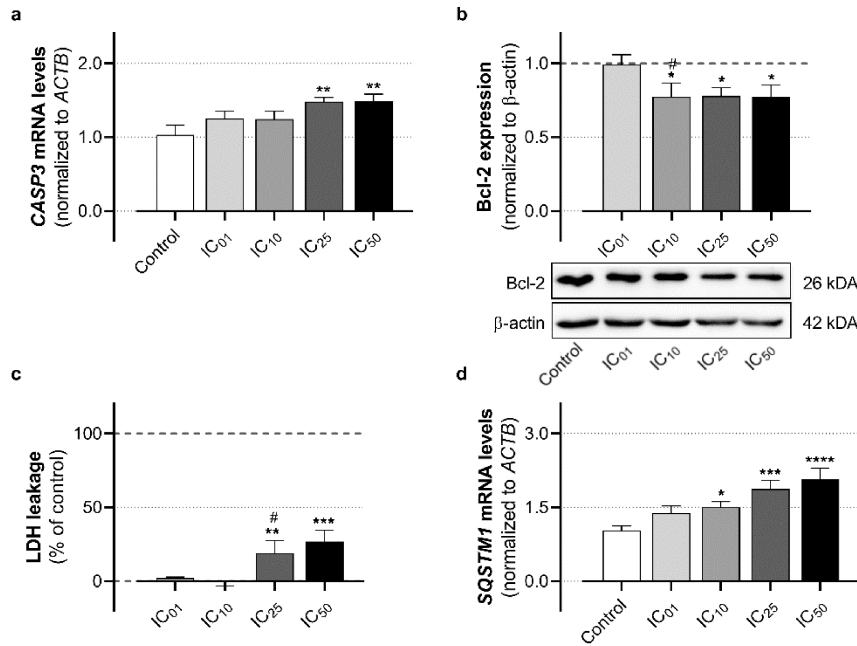


Fig. 5 Effect of Gd (III) on (a) *CASP3* mRNA levels and (b) Bcl-2 protein expression, (c) LDH leakage, and (d) *SQSTM1* mRNA levels in HK-2 cells exposed to different ICs of GdCl₃·6H₂O, for 24 h, at 37 °C. Data are presented as mean ± SEM of at least 5 independent experiments. * $p < 0.05$, ** $p < 0.01$, *** $p < 0.001$, **** $p < 0.0001$ vs. control; # $p < 0.05$ vs. previous IC. IC: inhibitory concentration; *CASP3*: caspase 3; Bcl-2: B-cell lymphoma 2; LDH: lactate dehydrogenase; *SQSTM1*: sequestosome-1.

Gd (III) interferes with renal lipid metabolism

As depicted in **Fig. 6**, double staining with BODIPY™ 493/503 and Hoechst 33342 revealed the presence of a large number of neutral lipid droplets in Gd (III)-exposed cells, localized outside the nuclei (stained blue on right panels; pink arrows). These vesicles, which were scarce in control cells (**Fig. 6a**), were already evident at the subtoxic concentration (**Fig. 6b**), and were apparently dispersed near the cell membrane, which is more perceptible at higher concentrations (**Figs. 6c, 6d** and **6e**). Of note, large vesicles with non-lipidic content (not stained with BODIPY™ 493/503) were noted at the two highest ICs tested, especially at the IC₅₀, as evidenced in the lower left part of **Fig. 6e**.

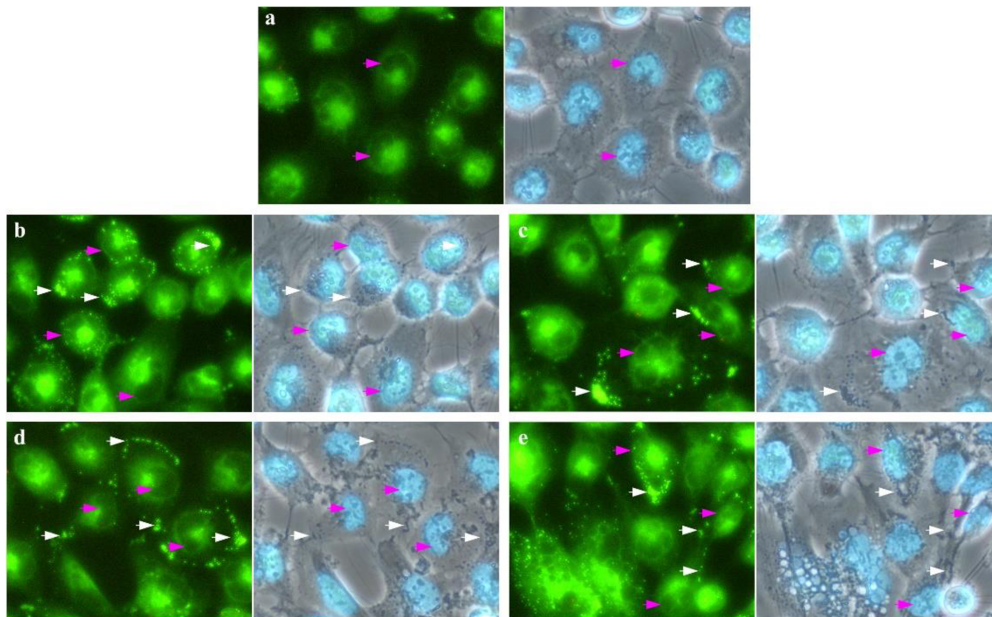


Fig. 6 Representative fluorescence microscopy images of BODIPY™ 493/503/Hoechst 33342 double staining of **(a)** control HK-2 cells, and cells exposed to **(b)** IC₀₁, **(c)** IC₁₀, **(d)** IC₂₅ and **(e)** IC₅₀ GdCl₃·6H₂O for 24 h, at 37°C. White arrows indicate neutral lipid droplets-stained bright green, while pink arrows evidence the localization of cells' nuclei, which are stained blue. Original magnification of 200×. IC: inhibitory concentration.

The impact of Gd (III) on the renal lipid metabolism was further investigated through the evaluation of the expression of the genes encoding for acetyl-CoA carboxylase 1 (*ACACA*), which catalyses the first step of fatty acid biosynthesis, and for the mitochondrial membrane-bound, lipid shuttling enzyme carnitine palmitoyltransferase 1A (*CPT1A*). Exposure of cells to Gd (III) lead to an upregulation of *ACACA*, which was significant already at the IC₁₀, with an expression of 1.4 ± 0.1 (vs. 1.0 ± 0.1 in control, $p < 0.01$), and similar at the following concentrations (**Fig. 7a**). The cells appear to respond to this effect with a gradual upregulation of *CPT1A*, with a 2.5- and 2.7-fold increase in expression over control for IC₂₅ ($p < 0.05$) and IC₅₀ ($p < 0.01$), respectively (**Fig. 7b**).

As cellular trafficking organelles, the lysosomes are important modulators of lipid metabolism (Liu and Czaja 2013). Therefore, we further evaluated the lysosomal activity through the measurement of neutral red uptake by lysosomes. A significant increase on neutral red uptake was found for IC₁₀ and IC₂₅ of about 11.0 ($p < 0.01$) and 7.2 % over control ($p < 0.05$), respectively, while no significant differences were found for the subtoxic and the highest concentrations (**Fig. 7c**).

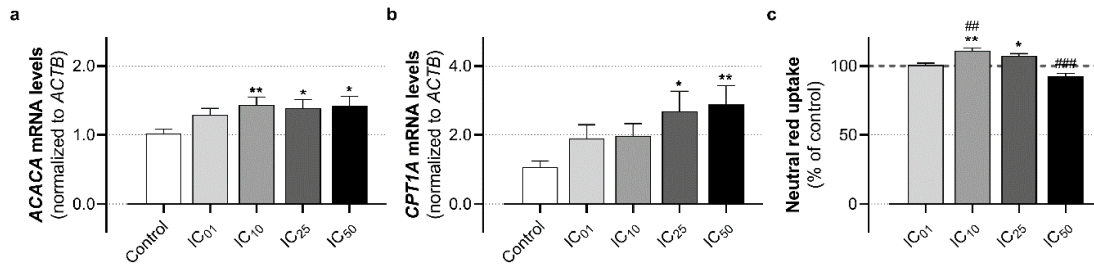


Fig. 7 Effect of Gd (III) on (a) *ACACA* mRNA levels, (b) *CPT1A* mRNA levels, and (c) neutral red uptake on HK-2 cells exposed to different ICs of GdCl₃·6H₂O for 24 h, at 37 °C. Data are presented as mean ± SEM of at least 6 independent experiments. * $p < 0.05$, ** $p < 0.01$ vs. control; ## $p < 0.01$, ### $p < 0.001$ vs. previous IC. IC: inhibitory concentration; *ACACA*: acetyl-CoA carboxylase 1; *CPT1A*: carnitine palmitoyltransferase 1A.

Gd (III) elicits multiple pathophysiological responses

Signaling pathways that, directly or indirectly, underlie the development of oxidative stress, mitochondrial dysfunction, apoptosis, necrosis and autophagy of renal cells, may trigger or result from other pathophysiological responses, such as inflammation or hypoxia responses, and fibrosis (Che et al. 2014). As depicted in Fig. 8, Gd (III) appears to trigger an inflammatory response in HK-2 cells, as shown by the upregulation of the pro-inflammatory genes *NFKB1* (Fig. 8a) and *IL6* (Fig. 8b) at the two highest concentrations tested. Furthermore, at the subtoxic concentration, we observed a 1.6-fold increase in the protein expression of the p65 subunit of the NF-kappa-B (NFκB) transcription complex over control (Fig. 8c; $p < 0.01$). Bmal1, a transcription factor that modulates the circadian rhythm and controls numerous metabolic and homeostatic pathways in several organs, including the kidney (Nikolaeva et al. 2016), was also shown to be overexpressed in Gd (III)-exposed cells at the lowest concentrations, with a 1.7- and 1.9-fold increase over control for IC₀₁ ($p < 0.05$) and IC₁₀ ($p < 0.01$), respectively (Fig 8d). Gd (III) also triggered the upregulation of genes involved in the inflammatory/fibrotic response in the kidney (Liu et al. 2013), including *IL1B* (Fig. 8e), with a 2-fold increase at the IC₅₀ ($p < 0.01$), and *TGFBI* (Fig. 8f), showing a significant increase in expression at the IC₁₀ ($p < 0.05$). Considering the crosstalk between oxidative stress, inflammation, fibrosis and hypoxia in the kidney (Liu et al. 2017a), we also evaluated the regulation of hypoxia-related genes by Gd (III) in HK-2 cells, namely the hypoxia-responsive gene *OPN* (Hwang et al. 1994), encoding for osteopontin (OPN), and *HIF1A*, which encodes for the transcription factor hypoxia-inducible factor-1α (HIF-1α)

that regulates the cellular response to oxygen levels (Shu et al. 2019). As depicted in **Fig. 8g**, *OPN* mRNA levels were already significantly increased at the lowest concentration (1.6 ± 0.1 vs. 1.0 ± 0.1 in control, $p < 0.01$) and remained upregulated at all other ICs, whereas *HIF1A* was only significantly overexpressed at the two highest concentrations, with a 1.6- and a 1.8-fold increase over control for IC₂₅ ($p < 0.05$) and IC₅₀ ($p < 0.01$), respectively (**Fig 8h**).

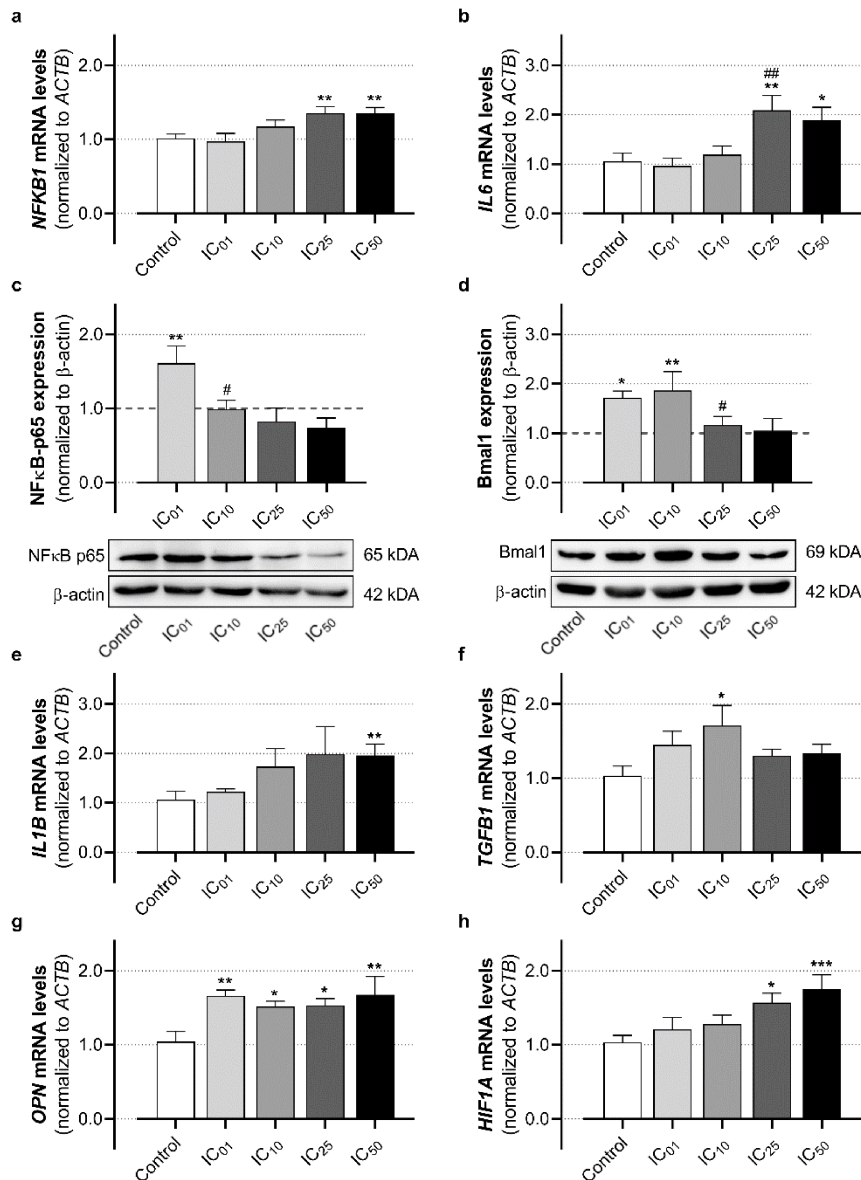


Fig. 8 Effect of Gd (III) on the expression of (a) *NFKB1*, (b) *IL6*, (c) NFκB-p65 protein, (d) Bmal1 protein, (e) *IL1B*, (f) *TGFBI*, (g) *OPN* and (h) *HIF1A* on HK-2 cells exposed to different ICs of GdCl₃·6H₂O, for 24 h, at 37 °C. Data are presented as mean ± SEM of at least 5 independent experiments run in duplicates. * $p < 0.05$, ** $p < 0.01$, *** $p < 0.001$ vs. control; # $p < 0.05$, ### $p < 0.01$ vs. previous IC. IC: inhibitory concentration; *NFKB1*: nuclear factor-kappa B subunit 1; *IL6*: interleukin-6; NFκB: nuclear factor-kappa B; Bmal1: brain and muscle aryl hydrocarbon receptor

nuclear translocator-like protein 1; *IL1B*: interleukin-1 beta; *TGFBI*: transforming growth factor beta 1; *OPN*: osteopontin; *HIF1A*: hypoxia-inducible factor-1 alpha.

Discussion

Gd (III) is currently used in the form of chelates in MRI, as a paramagnetic contrast media agent (Do et al. 2020). Over the years, several contrast agents have shown deleterious effects towards the kidney, in particular iodinated media (Faucon et al. 2019). Until recently, GBCA were considered safer alternatives to iodinated agents, entailing apparent low risk of adverse effects. However, recent evidence supports a close association of the use of these agents with toxic effects targeting different tissues and organs (Rogosnitzky and Branch 2016), which are particularly exacerbated in the kidney, especially in patients with renal impairment (Martino et al. 2021), and may even promote the development of NSF (Grobner 2006).

GBCA long-term toxicity has been attributed, at least partially, to the slow release of ionic Gd (III) from tissue deposits found in the brain, bone, skin, liver and kidney, into the bloodstream (Damme et al. 2020; Do et al. 2014; Do et al. 2020; Kanda et al. 2014; Mercantepe et al. 2018). However, it remains unclear which amount of Gd (III) may actually be released from the chelates, and at what extent free Gd (III) reaches and is accumulated in the tissues. Nevertheless, toxic potential of either Gd (III) and GBCA were already demonstrated in several *in vitro* models, including renal cells, central nervous system models, immune and vascular cells, and liver mitochondria (Rogosnitzky and Branch 2016). The underlying mechanisms of Gd (III) toxicity are still poorly clarified, and their identification might be crucial for outlining strategies to minimize adverse effects, particularly in the more vulnerable individuals. Importantly, Gd (III) is currently the only heavy metal suitable for MRI enhancement, and it is vital for diagnosis, staging and monitoring of disease treatment.

In the present study, we aimed at unveiling the mechanisms involved in the renal toxicity of Gd (III), resorting to the well-established cell line of human normal tubular proximal epithelial cells, HK-2 (Ryan et al. 1994). A complete concentration-response curve (MTT reduction assay) was obtained in HK-2 cells exposed to $GdCl_3 \cdot 6H_2O$ for 24 h, at concentrations ranging from nano to millimolar levels (500 nM – 100 mM); the estimated ICs eliciting 1, 10, 25 and 50 % of cell death were achieved at micromolar levels (3.4,

37.8, 113.5 and 340.5 μM , respectively) (**Fig. 1a**). The loss of cell viability was also time-dependent, with a significant aggravation from 24 to 48 h of exposure to the IC_{25} (**Fig. 1b**). On the other hand, no significant differences were noted up to 8 h of incubation with this IC, which may be indicative of relatively low acute cytotoxicity from Gd (III) in the proximal tubular epithelium. Nevertheless, it is important to note that the deposition of Gd (III)-rich precipitates in the renal proximal tubule of GBCA-exposed mice was recently reported by Do et al. (2020), which may render the proximal tubular cells more vulnerable to chronic/long-term cytotoxic effects.

Cell death induced by Gd (III) and GBCA in non-renal *in vitro* models has been associated to an aggravation of the intracellular oxidative status, characterized by increased formation of reactive oxygen species (ROS), depletion of the primary cellular antioxidant resource GSH, upregulation of endoplasmic reticulum stress markers and peroxidation of membrane lipid bilayers (Akhtar et al. 2020; Feng et al. 2010; Weng et al. 2018; Xia et al. 2011). Accordingly, we showed that Gd (III)-exposed HK-2 cells presented a decline in TAS at the two highest ICs tested, which was accompanied by a concentration-dependent decrease in GSH levels and a matching GSSG rise (**Fig. 2a** and **2b**). GSH homeostasis is modulated by both cell redox state and GSH *de novo* synthesis, and both processes are regulated by the Nrf2 transcription factor (Harvey et al. 2009; Steele et al. 2013). In fact, we found that these changes in GSH and GSSG levels elicited by Gd (III) exposure were accompanied by the upregulation of *NRF2*, reaching statistical significance at the IC_{50} (**Fig. 2c**). Our results suggest that the proximal tubular cells may be able to respond to the injury, even at such high concentrations, though it may be insufficient to counteract the established oxidative damage and/or avoid the deterioration of the antioxidant defenses of the cell. Nevertheless, since the observed increase in *NRF2* mRNA expression may not translate into an actual increase in protein activation, additional studies are required to confirm the postulated mechanism.

Besides its antioxidant properties, it is well known that GSH can bind to some metals at different coordination sites, with the sulfhydryl group presenting the highest affinity for cationic metals (Lushchak 2012). Garg et al. (2003) demonstrated the potential of trivalent lanthanides, including Gd (III), to form relatively stable complexes with GSH in aqueous solution. Therefore, we cannot discard the formation of Gd (III)-GSH adducts *in vitro* as a possible cause, at least to some extent, for the observed decline in GSH levels.

While increased ROS generation may lead to profound functional changes in the mitochondria, damaged mitochondria are also well-known sources of ROS generation. This interplay between oxidative stress and mitochondrial (dys)function is particularly important in renal tubular cells, which have high energetic demands and, thus, are rich in mitochondria (Gyuraszova et al. 2020). Pathological stimulus, such as increased oxidative stress, causes Ca^{2+} influx from the extracellular environment and from the endoplasmic reticulum into the cytoplasm, and further undergoes $\Delta\Psi\text{m}$ -dependent mitochondrial uptake. Mitochondrial Ca^{2+} overload hinders the oxidative phosphorylation, and consequently the ATP production; it also triggers the opening of the mitochondrial permeability transition pore (mPTP), leading to loss of $\Delta\Psi\text{m}$ (Brookes et al. 2004). In line with this, and with similar findings in other non-renal models (Rogosnitzky and Branch 2016), we found that Gd (III) induces mitochondrial dysfunction on proximal tubular cells, as shown by the rise in intracellular calcium, followed by mitochondrial membrane depolarization and ATP depletion at higher concentrations (**Fig. 3**).

The opening of the mPTP is a well-established hallmark of apoptosis, enabling the release of cytochrome *c* and the initiation of a signaling pathway that culminates in the activation of effector caspase 3 (Redza-Dutordoir and Averill-Bates 2016). Accordingly, we showed that the Gd (III)-induced death in HK-2 cells was portrayed by morphological changes consistent with apoptotic activation (**Fig. 4b** and **4c**), accompanied by the upregulation of *CASP3* (**Fig. 5a**), and decreased expression, already at the IC_{10} , of the Bcl-2 protein (**Fig. 5b**), which is an antagonist of pro-apoptotic modulators. At higher concentrations, we observed morphological features of necrotic cell death (**Fig. 4d** and **4e**), and a significant increase in LDH leakage at IC_{25} and IC_{50} (**Fig. 5c**). Since ATP is a major regulator of the switch in cell death mechanisms from apoptosis to necrosis (Nicotera and Melino 2004), it was reasonable to expect its occurrence once the cells become depleted of energy. Similar results were reported in rat cortical neurons, with loss of mitochondrial metabolic activity preceding ATP depletion, cytochrome *c* release, increased caspase 3 protein expression and rise in LDH release (Feng et al. 2010), which substantiates the activation of comparable mechanisms of cytotoxicity by Gd (III) in different target organs. Besides its anti-apoptotic role, Bcl-2 is also a modulator of autophagic cell death/survival, exerting an inhibitory effect by interacting with the pro-autophagic protein Beclin 1 and preventing the assembling of the pre-autophagosomal structure, thus inhibiting autophagy (Marquez and Xu 2012). Therefore, it was likely that the decrease

in the expression of the Bcl-2 protein, triggered by Gd (III) in renal cells, would have a positive impact in the activation of autophagy. Accordingly, we observed large vesicles with non-lipidic content, more evident at higher concentrations of Gd (III), which we hypothesize to be autophagosomes (**Fig. 6e**). Strengthening this hypothesis, we found that Gd (III) exposure led to a concentration-dependent upregulation of *SQSTM1* (**Fig. 5d**), the gene encoding for p62, a key protein in the autophagic initiation, reported to disrupt the Bcl-2:Beclin 1 interaction (Zhou et al. 2013). Our data comes in line with recent evidences of autophagic activation on human umbilical vein endothelial cells exposed to Gd (III) oxide nanoparticles (Akhtar et al. 2020). Although autophagy is known to trigger or inhibit cell death, depending on the cell type and involving environment, Takanezawa et al. (2020) have recently demonstrated that this programmed signaling pathway appears to exert a cytoprotective effect against Gd (III) in a human embryonic kidney cell line. Therefore, we postulate that the Gd (III)-exposed proximal tubular cells may be triggering autophagy to suppress the exacerbated oxidative damage. Additionally, we showed a rise in lysosomal activity (**Fig 7C**), despite the loss in cell viability (MTT reduction and LDH leakage assays), which is not only a key component of the process of degradation of damaged organelles and proteins through autophagy (Yun et al. 2020), but has also been implicated in lysosome-based lipid droplet degradation, in an autophagic process called lipophagy (Liu and Czaja 2013). The accumulation of cytoplasmic lipid droplets as a response to stress conditions has been gaining attention in the past years. Recent studies support their key role in the management of multiple signaling pathways involved in the redox homeostasis and programmed cell death (apoptosis and autophagy), going far beyond fatty acid storage and lipid metabolism regulation (Geltinger et al. 2020; Jarc and Petan 2019). Do et al. (2020) showed lipid-like droplets in the renal cortex cells, and particularly in the proximal tubule, of mice exposed to GBCA, which comes in line with the reported *in vivo* GBCA-induced dyslipidemia and disruption of the renal lipid metabolism (Do et al. 2019). Accordingly, we also showed the increase in neutral lipid-containing vesicles in Gd (III)-exposed HK-2 cells (**Fig. 6**). This is particularly important, as renal lipotoxicity appears to be a critical risk factor for the development of kidney disease (Izquierdo-Lahuerta et al. 2016). Though lipid droplet formation may be triggered as a defense mechanism against lipid peroxidation following oxidative damage (Jarc and Petan 2019), we also showed that Gd (III) may also elicit the biosynthesis of fatty acids, as demonstrated by the upregulation of *ACACA* (**Fig. 7a**), further fueling their storage.

On the other hand, exposed cells also overexpressed *CPT1A* (**Fig. 7b**), the encoding gene for the rate-limiting enzyme for fatty acid oxidation, CPT1A. Interestingly, CPT1A overexpression in the renal tubule of animals with renal fibrosis showed multiple protective effects, from blunted profibrotic and proinflammatory responses, to restored bioenergetic homeostasis (Miguel et al. 2021). Our results on *CPT1A* expression, along with the observed increase in lysosomal activation, essential for the process of lipolysis, substantiate the ability of the proximal tubular cells to counteract Gd (III)-induced renal lipid metabolism disruption, even at high levels of this metal. Nevertheless, this protective response appears to be insufficient to maintain the cells' energetic homeostasis, as evidenced by the observed ATP depletion, most likely due to the extensive mitochondrial damage at higher concentrations of Gd (III).

A growing amount of evidence substantiates a protective role for autophagy in the kidney under pathological conditions, being triggered by all sorts of cellular responses, including inflammation, fibrosis and hypoxia (Tang et al. 2020). In fact, the exposure of HK-2 cells to Gd (III) induced a pro-inflammatory response, as shown by the upregulation of *NFKB1* and *IL6* at the highest concentrations tested and, most importantly, by the increased expression of the NFκB-p65 protein at the subtoxic concentration, whose activation is involved in the upregulation of several genes related to mediators of cell death and proliferation, chemokines and inflammatory cytokines (Giridharan and Srinivasan 2018) (**Fig. 8a, 8b and 8c**). Recently, Weng et al. (2018) showed that macrophage exposure to subtoxic, physiologically relevant concentrations of GBCA triggers a pro-inflammatory reaction, which was exacerbated when there was a preexisting inflammatory state. Moreover, *in vivo* administration of GBCA showed that Gd (III) deposition in the brain is increased in areas of high inflammatory activity (Wang et al. 2019). This is particularly worrying, considering that GBCA-administration is used in MRI to improve the detection of pathologic conditions associated with inflammation, such as cancer.

The circadian clock controls many of the kidney's vital metabolic and homeostatic functions, including blood pressure regulation and glomerular filtration rate (Firsov and Bonny 2018). Furthermore, the circadian rhythm also appears to modulate drug availability, cell's metabolome, as well as the cellular immune response through the *BMAL1* gene (Early et al. 2018; Nikolaeva et al. 2016; Wang et al. 2020; Yu et al. 2019). We showed that Gd (III) elicited a significant rise in Bmal1 protein expression at the two

lowest ICs tested (**Fig. 8d**), which may potentiate the effects associated to the role of circadian clock in different cellular processes that appear to be disturbed in Gd (III) exposed HK-2 cells. In fact, in a recent study using HK-2 cells, *BMAL1* was shown to mediate cisplatin-induced renal damage, and appeared to further potentiate renal hepatization (acute upregulation in renal cortex of genes commonly expressed only in the liver, as a consequence of ischemic/toxic damage) (Zha et al. 2020), a phenomenon described in acute kidney injury (Zager et al. 2012). A recent work by Early et al. (2018), showed that *Bmal1* directly regulates the expression of *Nrf2* in macrophages, playing a critical role in the immune response to oxidative damage. In their study, *BMAL1* deletion resulted in increased production of the pro-inflammatory cytokine interleukin-1 beta ($IL-1\beta$) and of the hypoxic response protein, *HIF-1 α* . In line with this, we found that for higher levels of Gd (III), at which the protein expression of *Bmal1* returns to control levels and the upregulation of pro-inflammatory genes (*NFKB1* and *IL6* at IC_{25} and IC_{50}) have already occurred, there was also an upregulation of both *IL1B* and *HIF1A* (**Fig. 8e** and **8h**), which supports the ability of Gd (III) to induce not only renal inflammation, but also tubular hypoxia, both hallmarks of chronic and acute kidney disease (Tanaka et al. 2014), and risk factors for renal fibrosis (Liu et al. 2017a). Interestingly, we found that *OPN* is upregulated by Gd (III) already at the lowest IC tested (**Fig. 8g**). *OPN* is a hypoxia-sensitive protein that has been implicated in many aspects of tumor progression, including in the upstream activation of *HIF1A* (Raja et al. 2014). In the kidney, *OPN* protein has been shown to regulate several signaling pathways involved in apoptosis, oxidative stress, inflammation, and tubulointerstitial and glomerular fibrosis (Merszei et al. 2010; Song et al. 2010; Wolak et al. 2009; Yoo et al. 2006). Regarding the fibrotic process, *OPN* promotes the production of transforming growth factor beta ($TGF-\beta$), which in turn drives myofibroblast differentiation and epithelial-to-mesenchymal transition (Lenga et al. 2008; Weber et al. 2012). Furthermore, a recent study by Lemos et al. (2018) showed that $IL-1\beta$ appears to be the link between inflammation and the initiation of renal fibrosis. In line with this, we found that, besides a significant increase in *IL1B* mRNA levels at the IC_{50} , *TGFB1* was also upregulated in Gd (III)-exposed HK-2 cells, but at lower levels (IC_{10}) (**Fig. 8f**).

It should be stressed that it is still difficult to establish pertinent concentrations to be tested *in vitro*, which is the major limitation of this study. In fact, the amount of Gd (III) that may be released from administered GBCA, as well as the portion of this circulating metal

that undergoes bioaccumulation in the kidney, relies on multiple factors, including type (ionic linear, nonionic linear, or macrocyclic) or brand of agent used, dose, administration route, number of administrations, and pre-existing comorbidities (e.g. inflammation and renal dysfunction exacerbate tissue deposition). However, data available from case-reports and pharmacokinetic studies can give us some insights on this matter. For instance, Ringler et al. (2021) found median serum and urine levels of Gd (III) up to 34.7 and 23,820 $\mu\text{g}/\text{mL}$, respectively, 1 h after an intra-articular injection of GBCA in a rat model. Serum levels of Gd (III) ranging from 0.6 to 277.8 ng/mL were found in NSF patients (Christensen et al. 2011; Nehra et al. 2018), while a median peak plasma level of 65.7 $\mu\text{g}/\text{mL}$ was estimated in a group of children with normal renal function exposed to a linear GBCA (Pirovano et al. 2015). Animal studies show levels ranging from 200 ng to over 100 μg of Gd (III) per gram of kidney tissue after a single administration of a GBCA (Acar et al. 2019; Haylor et al. 2010; Ringler et al. 2021), and levels up to 5 $\mu\text{mol}/\text{g}$ (around 785 $\mu\text{g}/\text{g}$) in a rat model of NSF (Haylor et al. 2012). In a case-report of a patient with renal failure diagnosed with NSF, the autopsy findings showed Gd (III) levels of 488.2 to 585.4 parts per million (or $\mu\text{g}/\text{g}$) in the kidneys (Kay et al. 2008). Therefore, we can only postulate that the hereby tested concentrations may comprise pathophysiologically relevant levels of Gd (III) (resulting from a standard administration of GBCA) in the proximal tubule. Additionally, the exposure to a low-to-high concentration range of Gd (III) aims at establishing a concentration-effect relation in a mechanistic point-of-view, which may implicate the selection of concentrations that may not be attained pathophysiologically. Finally, a mechanistic study conducted at different time-points is essential to fully establish an unequivocal sequence of events and/or signaling pathways that may underlie the adverse effects of Gd (III) in renal cells. Thus, further studies are required to confirm the herein presented hypotheses.

Many efforts have been made over the years to minimize the risks entailed by these agents, including the development of more stable complexes, the restriction of linear agents, and the reduction of doses for renal patients. Nevertheless, the number of reports on GBCA-induced toxicity keeps rising. Our data, as summarized in **Table 2**, supports the potential of Gd (III) to trigger a multiplicity of pathophysiological responses in the proximal tubule, even at low levels. Besides adding valuable information to the growing body of evidence on GBCA toxicity, this work further supports the need to develop stronger chelators and to limit their use to situations in which the benefits greatly

outweigh the risks. Overall, Gd (III) nephrotoxicity appears to involve signaling pathways that are common to other affected organs. By establishing the cellular and molecular mechanisms underlying the toxicity of Gd (III), these pathways and their modulators could be viewed as potential targets to minimize the adverse effects of GBCA exposure, or even as biomarkers for an early detection of GBCA-induced nephrotoxicity, allowing a timely intervention. The identification of the triggered cellular responses in different organs could further guide the restriction of GBCA use in patients with pre-existent disorders that involve such responses, such as diseases linked to inflammation and oxidative stress.

Table 2: Summary of the signaling pathways affected by a 24-h exposure of HK-2 cells to GdCl₃·6H₂O, and variation of the assessed markers at each IC tested

Affected pathway	Altered marker	GdCl ₃ ·6H ₂ O			
		IC ₀₁	IC ₁₀	IC ₂₅	IC ₅₀
<i>Oxidative stress</i>	↓ TAS	-	-	+	+
	↑ GSSG	-	+	+	+
	↓ GSH	-	-	+	+
	↑ <i>NRF2</i>	-	-	-	+
<i>Mitochondrial function</i>	↑ intracellular calcium	-	-	+	+
	↓ ΔΨ _m	-	-	-	+
	↓ ATP	-	-	+	+
<i>Apoptosis</i>	↑ <i>CASP3</i>	-	-	+	+
	↓ Bcl-2	-	+	+	+
<i>Necrosis</i>	↑ LDH leakage	-	-	+	+
<i>Autophagy</i>	↑ <i>SQSTM1</i>	-	+	+	+
<i>Lipid metabolism</i>	↑ Lipid droplets	+	+	+	+
	↑ <i>ACACA</i>	-	+	+	+
	↑ <i>CPT1A</i>	-	-	+	+
	↑ neutral red uptake	-	+	+	-
<i>Inflammation</i>	↑ <i>NFKB1</i>	-	-	+	+
	↑ <i>IL6</i>	-	-	+	+
	↑ NFκB-p65	+	-	-	-
<i>Fibrosis</i>	↑ <i>IL1B</i>	-	-	-	+
	↑ <i>TGFBI</i>	-	+	-	-
<i>Hypoxia</i>	↑ <i>OPN</i>	+	+	+	+
	↑ <i>HIF1A</i>	-	-	+	+
<i>Circadian rhythm</i>	↑ Bmal1	+	+	-	-

IC: inhibitory concentration; TAS: total antioxidant status; GSH: reduced glutathione; GSSG: oxidized glutathione; *NRF2*: nuclear factor erythroid-2-related factor 2; ΔΨ_m: mitochondrial membrane potential; ATP: adenosine triphosphate; *CASP3*: caspase 3; Bcl-2: B-cell lymphoma 2; LDH: lactate dehydrogenase; *SQSTM1*: sequestosome-1; *ACACA*: acetyl-CoA carboxylase 1; *CPT1A*: carnitine palmitoyltransferase 1A; *NFKB1*: nuclear factor-kappa B subunit 1; *IL6*: interleukin-6; NFκB: nuclear factor-kappa B; *IL1B*: interleukin-1 beta; *TGFBI*: transforming growth factor beta

1; *OPN*: osteopontin; *HIF1A*: hypoxia-inducible factor-1 alpha; *Bmal1*: brain and muscle aryl hydrocarbon receptor nuclear translocator-like protein 1.

Conclusions

GBCA use in MRI leads to a great variety of toxic effects that are exacerbated in patients with pre-existing renal damage and/or inflammatory conditions. Our work showed that, even at low levels, Gd (III) has the potential to trigger an intricate deleterious response in the renal proximal tubule that encompasses multiple risk factors that are known to underlie the development and progression of renal disease. Therefore, the risk-benefit balance of the clinical use of this type of contrast agents deserves further review, considering not only their toxicity towards renal patients, but also their potential as triggers of renal disease.

Conflicts of interest

The authors declare that there are no conflicts of interest.

Funding

This work was financed by national funds from FCT - Fundação para a Ciência e a Tecnologia, I.P., in the scope of the project UIDP/04378/2020 and UIDB/04378/2020 of the Research Unit on Applied Molecular Biosciences - UCIBIO and the project LA/P/0140/2020 of the Associate Laboratory Institute for Health and Bioeconomy - i4HB. S. Rocha also acknowledges FCT/MCTES (PTDC/MEC-CAR/31322/2017) and FEDER/COMPETE 2020 (POCI-01-0145-FEDER-031322) for her Researcher contract.

Authors' contributions

A.S.S, S.C. and M.J.V. conceived and designed the study. N.R.S, S.R. and M.J.V. collected and analysed data. All authors contributed for the discussion of data, and manuscript drafting and revision.

References

- Acar T, Kaya E, Yoruk MD, Duzenli N, Senturk RS, Can C, Ozturk L, Tomruk C, Uyanikgil Y, Rybicki FJ. 2019. Changes in tissue gadolinium biodistribution measured in an animal model exposed to four chelating agents. *Jpn J Radiol.* 37(6):458-465.
- Akhtar MJ, Ahamed M, Alhadlaq H. 2020. Gadolinium oxide nanoparticles induce toxicity in human endothelial huvecs via lipid peroxidation, mitochondrial dysfunction and autophagy modulation. *Nanomaterials (Basel).* 10(9).
- Benzie IF, Strain JJ. 1996. The ferric reducing ability of plasma (frap) as a measure of "antioxidant power": The frap assay. *Anal Biochem.* 239(1):70-76.
- Bernas T, Dobrucki J. 2002. Mitochondrial and nonmitochondrial reduction of mtt: Interaction of mtt with tmre, jc-1, and nao mitochondrial fluorescent probes. *Cytometry.* 47(4):236-242.
- Brookes PS, Yoon Y, Robotham JL, Anders MW, Sheu SS. 2004. Calcium, atp, and ros: A mitochondrial love-hate triangle. *Am J Physiol Cell Physiol.* 287(4):C817-833.
- Bussi S, Coppo A, Celeste R, Fanizzi A, Fringuello Mingo A, Ferraris A, Botteron C, Kirchin MA, Tedoldi F, Maisano F. 2020. Macrocyclic mr contrast agents: Evaluation of multiple-organ gadolinium retention in healthy rats. *Insights Imaging.* 11(1):11.
- Che R, Yuan Y, Huang S, Zhang A. 2014. Mitochondrial dysfunction in the pathophysiology of renal diseases. *Am J Physiol Renal Physiol.* 306(4):F367-378.
- Christensen KN, Lee CU, Hanley MM, Leung N, Moyer TP, Pittelkow MR. 2011. Quantification of gadolinium in fresh skin and serum samples from patients with nephrogenic systemic fibrosis. *J Am Acad Dermatol.* 64(1):91-96.
- Clases D, Fingerhut S, Jeibmann A, Sperling M, Doble P, Karst U. 2019. La-icp-ms/ms improves limits of detection in elemental bioimaging of gadolinium deposition originating from mri contrast agents in skin and brain tissues. *J Trace Elem Med Biol.* 51:212-218.
- Crowley LC, Christensen ME, Waterhouse NJ. 2016. Measuring mitochondrial transmembrane potential by tmre staining. *Cold Spring Harb Protoc.* 2016(12).
- Damme NM, Fernandez DP, Wang LM, Wu Q, Kirk RA, Towner RA, McNally JS, Hoffman JM, Morton KA. 2020. Analysis of retention of gadolinium by brain, bone, and blood following linear gadolinium-based contrast agent administration in rats with experimental sepsis. *Magn Reson Med.* 83(6):1930-1939.
- Dekkers IA, Roos R, van der Molen AJ. 2018. Gadolinium retention after administration of contrast agents based on linear chelators and the recommendations of the european medicines agency. *Eur Radiol.* 28(4):1579-1584.
- Dias da Silva D, Ferreira B, Roque Bravo R, Rebelo R, Duarte de Almeida T, Valente MJ, Silva JP, Carvalho F, Bastos ML, Carmo H. 2019. The new psychoactive substance 3-methylmethcathinone (3-mmh or methedrone) induces oxidative stress, apoptosis, and autophagy in primary rat hepatocytes at human-relevant concentrations. *Arch Toxicol.* 93(9):2617-2634.
- Do C, Barnes JL, Tan C, Wagner B. 2014. Type of mri contrast, tissue gadolinium, and fibrosis. *Am J Physiol Renal Physiol.* 307(7):F844-855.
- Do C, DeAguero J, Brearley A, Trejo X, Howard T, Escobar GP, Wagner B. 2020. Gadolinium-based contrast agent use, their safety, and practice evolution. *Kidney360.10.34067/KID.0000272019.*
- Do C, Ford B, Lee DY, Tan C, Escobar P, Wagner B. 2019. Gadolinium-based contrast agents: Stimulators of myeloid-induced renal fibrosis and major metabolic disruptors. *Toxicol Appl Pharmacol.* 375:32-45.
- Early JO, Menon D, Wyse CA, Cervantes-Silva MP, Zaslona Z, Carroll RG, Palsson-McDermott EM, Angiari S, Ryan DG, Corcoran SE et al. 2018. Circadian clock protein bmal1 regulates il-1beta in macrophages via nrf2. *Proc Natl Acad Sci U S A.* 115(36):E8460-E8468.
- Eggleston H, Panizzi P. 2014. Molecular imaging of bacterial infections in vivo: The discrimination of infection from inflammation. *Informatics (MDPI).* 1(1):72-99.
- Eguchi Y, Shimizu S, Tsujimoto Y. 1997. Intracellular atp levels determine cell death fate by apoptosis or necrosis. *Cancer research.* 57(10):1835-1840.
- Elmstahl B, Nyman U, Leander P, Chai CM, Golman K, Bjork J, Almen T. 2006. Gadolinium contrast media are more nephrotoxic than iodine media. The importance of osmolality in direct renal artery injections. *Eur Radiol.* 16(12):2712-2720.
- Faucon AL, Bobrie G, Clement O. 2019. Nephrotoxicity of iodinated contrast media: From pathophysiology to prevention strategies. *Eur J Radiol.* 116:231-241.
- Feng X, Xia Q, Yuan L, Yang X, Wang K. 2010. Impaired mitochondrial function and oxidative stress in rat cortical neurons: Implications for gadolinium-induced neurotoxicity. *Neurotoxicology.* 31(4):391-398.



- Firsov D, Bonny O. 2018. Circadian rhythms and the kidney. *Nat Rev Nephrol.* 14(10):626-635.
- Garcia J, Liu SZ, Louie AY. 2017. Biological effects of mri contrast agents: Gadolinium retention, potential mechanisms and a role for phosphorus. *Philos Trans A Math Phys Eng Sci.* 375(2107).
- Garg B, Singh B, Kumar DN, Singh P. 2003. Thermodynamic parameters and stability constants of lanthanide (iii) complexes of biologically active glutathione (gsh) and their chemical speciation.
- Geltinger F, Schartel L, Wiederstein M, Tevini J, Aigner E, Felder TK, Rinnerthaler M. 2020. Friend or foe: Lipid droplets as organelles for protein and lipid storage in cellular stress response, aging and disease. *Molecules.* 25(21).
- Giridharan S, Srinivasan M. 2018. Mechanisms of nf-kappab p65 and strategies for therapeutic manipulation. *J Inflamm Res.* 11:407-419.
- Grobner T. 2006. Gadolinium--a specific trigger for the development of nephrogenic fibrosing dermopathy and nephrogenic systemic fibrosis? *Nephrol Dial Transplant.* 21(4):1104-1108.
- Gyuraszova M, Gurecka R, Babickova J, Tothova L. 2020. Oxidative stress in the pathophysiology of kidney disease: Implications for noninvasive monitoring and identification of biomarkers. *Oxid Med Cell Longev.* 2020:5478708.
- Harvey CJ, Thimmulappa RK, Singh A, Blake DJ, Ling G, Wakabayashi N, Fujii J, Myers A, Biswal S. 2009. Nrf2-regulated glutathione recycling independent of biosynthesis is critical for cell survival during oxidative stress. *Free Radic Biol Med.* 46(4):443-453.
- Haylor J, Dencausse A, Vickers M, Nutter F, Jestin G, Slater D, Idee JM, Morcos S. 2010. Nephrogenic gadolinium biodistribution and skin cellularity following a single injection of omniscan in the rat. *Invest Radiol.* 45(9):507-512.
- Haylor J, Schroeder J, Wagner B, Nutter F, Jestin G, Idee JM, Morcos S. 2012. Skin gadolinium following use of mr contrast agents in a rat model of nephrogenic systemic fibrosis. *Radiology.* 263(1):107-116.
- Heinrich MC, Kuhlmann MK, Kohlbacher S, Scheer M, Grgic A, Heckmann MB, Uder M. 2007. Cytotoxicity of iodinated and gadolinium-based contrast agents in renal tubular cells at angiographic concentrations: In vitro study. *Radiology.* 242(2):425-434.
- Hwang SM, Wilson PD, Laskin JD, Denhardt DT. 1994. Age and development-related changes in osteopontin and nitric oxide synthase mrna levels in human kidney proximal tubule epithelial cells: Contrasting responses to hypoxia and reoxygenation. *J Cell Physiol.* 160(1):61-68.
- Izquierdo-Lahuerta A, Martinez-Garcia C, Medina-Gomez G. 2016. Lipotoxicity as a trigger factor of renal disease. *J Nephrol.* 29(5):603-610.
- Jarc E, Petan T. 2019. Lipid droplets and the management of cellular stress. *Yale J Biol Med.* 92(3):435-452.
- Kanda T, Ishii K, Kawaguchi H, Kitajima K, Takenaka D. 2014. High signal intensity in the dentate nucleus and globus pallidus on unenhanced t1-weighted mr images: Relationship with increasing cumulative dose of a gadolinium-based contrast material. *Radiology.* 270(3):834-841.
- Kay J, Bazari H, Avery LL, Koreishi AF. 2008. Case records of the massachusetts general hospital. Case 6-2008. A 46-year-old woman with renal failure and stiffness of the joints and skin. *N Engl J Med.* 358(8):827-838.
- Le Fur M, Caravan P. 2019. The biological fate of gadolinium-based mri contrast agents: A call to action for bioinorganic chemists. *Metallomics.* 11(2):240-254.
- Ledneva E, Karie S, Launay-Vacher V, Janus N, Deray G. 2009. Renal safety of gadolinium-based contrast media in patients with chronic renal insufficiency. *Radiology.* 250(3):618-628.
- Lei R, Zhao F, Tang CY, Luo M, Yang SK, Cheng W, Li XW, Duan SB. 2018. Mitophagy plays a protective role in iodinated contrast-induced acute renal tubular epithelial cells injury. *Cell Physiol Biochem.* 46(3):975-985.
- Lemos DR, McMurdo M, Karaca G, Wilflingseder J, Leaf IA, Gupta N, Miyoshi T, Susa K, Johnson BG, Soliman K et al. 2018. Interleukin-1beta activates a myc-dependent metabolic switch in kidney stromal cells necessary for progressive tubulointerstitial fibrosis. *J Am Soc Nephrol.* 29(6):1690-1705.
- Lenga Y, Koh A, Perera AS, McCulloch CA, Sodek J, Zohar R. 2008. Osteopontin expression is required for myofibroblast differentiation. *Circ Res.* 102(3):319-327.
- Levine B, Sinha SC, Kroemer G. 2008. Bcl-2 family members: Dual regulators of apoptosis and autophagy. *Autophagy.* 4(5):600-606.
- Liu GX, Li YQ, Huang XR, Wei L, Chen HY, Shi YJ, Heuchel RL, Lan HY. 2013. Disruption of smad7 promotes ang ii-mediated renal inflammation and fibrosis via sp1-tgf-beta/smad3-nf.Kappab-dependent mechanisms in mice. *PLoS One.* 8(1):e53573.
- Liu K, Czaja MJ. 2013. Regulation of lipid stores and metabolism by lipophagy. *Cell Death Differ.* 20(1):3-11.



- Liu M, Ning X, Li R, Yang Z, Yang X, Sun S, Qian Q. 2017a. Signalling pathways involved in hypoxia-induced renal fibrosis. *J Cell Mol Med.* 21(7):1248-1259.
- Liu N, Lei R, Tang MM, Cheng W, Luo M, Xu Q, Duan SB. 2017b. Autophagy is activated to protect renal tubular epithelial cells against iodinated contrast media-induced cytotoxicity. *Mol Med Rep.* 16(6):8277-8282.
- Livak KJ, Schmittgen TD. 2001. Analysis of relative gene expression data using real-time quantitative PCR and the $2^{-\Delta\Delta C_t}$ method. *Methods.* 25(4):402-408.
- Lushchak VI. 2012. Glutathione homeostasis and functions: Potential targets for medical interventions. *J Amino Acids.* 2012:736837.
- Ly JD, Grubb DR, Lawen A. 2003. The mitochondrial membrane potential ($\Delta\psi(m)$) in apoptosis; an update. *Apoptosis.* 8(2):115-128.
- Marquez RT, Xu L. 2012. Bcl-2:Beclin 1 complex: Multiple mechanisms regulating autophagy/apoptosis toggle switch. *Am J Cancer Res.* 2(2):214-221.
- Martino F, Amici G, Rosner M, Ronco C, Novara G. 2021. Gadolinium-based contrast media nephrotoxicity in kidney impairment: The physio-pathological conditions for the perfect murder. *J Clin Med.* 10(2).
- Mercantepe T, Tumkaya L, Celiker FB, Topal Suzan Z, Cinar S, Akyildiz K, Mercantepe F, Yilmaz A. 2018. Effects of gadolinium-based MRI contrast agents on liver tissue. *J Magn Reson Imaging.* 48(5):1367-1374.
- Merszei J, Wu J, Torres L, Hicks JM, Bartkowiak T, Tan F, Lou YH. 2010. Osteopontin overproduction is associated with progression of glomerular fibrosis in a rat model of anti-glomerular basement membrane glomerulonephritis. *Am J Nephrol.* 32(3):262-271.
- Miguel V, Tituana J, Herrero JI, Herrero L, Serra D, Cuevas P, Barbas C, Puyol DR, Marquez-Exposito L, Ruiz-Ortega M et al. 2021. Renal tubule *cpt1a* overexpression protects from kidney fibrosis by restoring mitochondrial homeostasis. *J Clin Invest.* 131(5).
- Murata N, Gonzalez-Cuyar LF, Murata K, Fligner C, Dills R, Hippe D, Maravilla KR. 2016. Macrocyclic and other non-group 1 gadolinium contrast agents deposit low levels of gadolinium in brain and bone tissue: Preliminary results from 9 patients with normal renal function. *Invest Radiol.* 51(7):447-453.
- Nehra AK, McDonald RJ, Bluhm AM, Gunderson TM, Murray DL, Jannetto PJ, Kallmes DF, Eckel LJ, McDonald JS. 2018. Accumulation of gadolinium in human cerebrospinal fluid after gadobutrol-enhanced MRI imaging: A prospective observational cohort study. *Radiology.* 288(2):416-423.
- Nicotera P, Melino G. 2004. Regulation of the apoptosis–necrosis switch. *Oncogene.* 23(16):2757-2765.
- Nikolaeva S, Ansermet C, Centeno G, Pradervand S, Bize V, Mordasini D, Henry H, Koesters R, Maillard M, Bonny O et al. 2016. Nephron-specific deletion of circadian clock gene *bmal1* alters the plasma and renal metabolome and impairs drug disposition. *J Am Soc Nephrol.* 27(10):2997-3004.
- Peng PA, Wang L, Ma Q, Xin Y, Zhang O, Han HY, Liu XL, Ji QW, Zhou YJ, Zhao YX. 2015. Valsartan protects HK-2 cells from contrast media-induced apoptosis by inhibiting endoplasmic reticulum stress. *Cell Biol Int.* 39(12):1408-1417.
- Pirovano G, Kirchin MA, Lorusso V, Patel R, Shen N. 2015. Pharmacokinetics of gadobenate dimeglumine in children 2 to 5 years of age undergoing MRI of the central nervous system. *J Magn Reson Imaging.* 41(4):1096-1103.
- Qiu B, Simon MC. 2016. Bodipy 493/503 staining of neutral lipid droplets for microscopy and quantification by flow cytometry. *Bio Protoc.* 6(17):1912.
- Raja R, Kale S, Thorat D, Soundararajan G, Lohite K, Mane A, Karnik S, Kundu GC. 2014. Hypoxia-driven osteopontin contributes to breast tumor growth through modulation of HIF1 α -mediated vegf-dependent angiogenesis. *Oncogene.* 33(16):2053-2064.
- Redza-Dutordoir M, Averill-Bates DA. 2016. Activation of apoptosis signalling pathways by reactive oxygen species. *Biochim Biophys Acta.* 1863(12):2977-2992.
- Ringler MD, Rhodes NG, Ayers-Ringler JR, Jakaitis DR, McDonald RJ, Kallmes DF, McDonald JS. 2021. Gadolinium retention within multiple rat organs after intra-articular administration of gadolinium-based contrast agents. *Skeletal Radiol.* 50(7):1419-1425.
- Rogosnitzky M, Branch S. 2016. Gadolinium-based contrast agent toxicity: A review of known and proposed mechanisms. *Biometals.* 29(3):365-376.
- Ryan MJ, Johnson G, Kirk J, Fuerstenberg SM, Zager RA, Torok-Storb B. 1994. HK-2: An immortalized proximal tubule epithelial cell line from normal adult human kidney. *Kidney Int.* 45(1):48-57.
- Shu S, Wang Y, Zheng M, Liu Z, Cai J, Tang C, Dong Z. 2019. Hypoxia and hypoxia-inducible factors in kidney injury and repair. *Cells.* 8(3).



- Song YR, You SJ, Lee YM, Chin HJ, Chae DW, Oh YK, Joo KW, Han JS, Na KY. 2010. Activation of hypoxia-inducible factor attenuates renal injury in rat remnant kidney. *Nephrol Dial Transplant.* 25(1):77-85.
- Steele ML, Fuller S, Patel M, Kersaitis C, Ooi L, Munch G. 2013. Effect of nrf2 activators on release of glutathione, cysteinylglycine and homocysteine by human u373 astroglial cells. *Redox Biol.* 1:441-445.
- Takanezawa Y, Nakamura R, Kusaka T, Ohshiro Y, Uraguchi S, Kiyono M. 2020. Significant contribution of autophagy in mitigating cytotoxicity of gadolinium ions. *Biochem Biophys Res Commun.* 526(1):206-212.
- Tanaka S, Tanaka T, Nangaku M. 2014. Hypoxia as a key player in the aki-to-ckd transition. *Am J Physiol Renal Physiol.* 307(11):F1187-1195.
- Tang C, Livingston MJ, Liu Z, Dong Z. 2020. Autophagy in kidney homeostasis and disease. *Nat Rev Nephrol.* 16(9):489-508.
- Valente MJ, Henrique R, Vilas-Boas V, Silva R, Bastos Mde L, Carvalho F, Guedes de Pinho P, Carvalho M. 2012. Cocaine-induced kidney toxicity: An in vitro study using primary cultured human proximal tubular epithelial cells. *Arch Toxicol.* 86(2):249-261.
- Wagner B, Drel V, Gorin Y. 2016. Pathophysiology of gadolinium-associated systemic fibrosis. *Am J Physiol Renal Physiol.* 311(1):F1-F11.
- Wang S, Hesse B, Roman M, Stier D, Castillo-Michel H, Cotte M, Suuronen JP, Lagrange A, Radbruch H, Paul F et al. 2019. Increased retention of gadolinium in the inflamed brain after repeated administration of gadopentetate dimeglumine: A proof-of-concept study in mice combining icp-ms and micro- and nano-sr-xrf. *Invest Radiol.* 54(10):617-626.
- Wang XL, Wolff SEC, Korpel N, Milanova I, Sandu C, Rensen PCN, Kooijman S, Cassel JC, Kalsbeek A, Boutillier AL et al. 2020. Deficiency of the circadian clock gene *bmal1* reduces microglial immunometabolism. *Front Immunol.* 11:586399.
- Weber CE, Li NY, Wai PY, Kuo PC. 2012. Epithelial-mesenchymal transition, tgf-beta, and osteopontin in wound healing and tissue remodeling after injury. *J Burn Care Res.* 33(3):311-318.
- Weng TI, Chen HJ, Lu CW, Ho YC, Wu JL, Liu SH, Hsiao JK. 2018. Exposure of macrophages to low-dose gadolinium-based contrast medium: Impact on oxidative stress and cytokines production. *Contrast Media Mol Imaging.* 2018:3535769.
- Wolak T, Kim H, Ren Y, Kim J, Vaziri ND, Nicholas SB. 2009. Osteopontin modulates angiotensin ii-induced inflammation, oxidative stress, and fibrosis of the kidney. *Kidney Int.* 76(1):32-43.
- Xia Q, Feng X, Huang H, Du L, Yang X, Wang K. 2011. Gadolinium-induced oxidative stress triggers endoplasmic reticulum stress in rat cortical neurons. *J Neurochem.* 117(1):38-47.
- Yoo KH, Thornhill BA, Forbes MS, Coleman CM, Marcinko ES, Liaw L, Chevalier RL. 2006. Osteopontin regulates renal apoptosis and interstitial fibrosis in neonatal chronic unilateral ureteral obstruction. *Kidney Int.* 70(10):1735-1741.
- Yu F, Zhang T, Zhou C, Xu H, Guo L, Chen M, Wu B. 2019. The circadian clock gene *bmal1* controls intestinal exporter *mrp2* and drug disposition. *Theranostics.* 9(10):2754-2767.
- Yun HR, Jo YH, Kim J, Shin Y, Kim SS, Choi TG. 2020. Roles of autophagy in oxidative stress. *Int J Mol Sci.* 21(9).
- Zager RA, Vijayan A, Johnson AC. 2012. Proximal tubule haptoglobin gene activation is an integral component of the acute kidney injury "stress response". *Am J Physiol Renal Physiol.* 303(1):F139-148.
- Zha M, Tian T, Xu W, Liu S, Jia J, Wang L, Yan Q, Li N, Yu J, Huang L. 2020. The circadian clock gene *bmal1* facilitates cisplatin-induced renal injury and hepatization. *Cell Death Dis.* 11(6):446.
- Zhang Q, Liu X, Li N, Zhang J, Yang J, Bu P. 2018. Sirtuin 3 deficiency aggravates contrast-induced acute kidney injury. *J Transl Med.* 16(1):313.
- Zhou L, Wang HF, Ren HG, Chen D, Gao F, Hu QS, Fu C, Xu RJ, Ying Z, Wang GH. 2013. Bcl-2-dependent upregulation of autophagy by sequestosome 1/p62 in vitro. *Acta Pharmacol Sin.* 34(5):651-656.
- Zhou Z, Lu ZR. 2013. Gadolinium-based contrast agents for magnetic resonance cancer imaging. *Wiley Interdiscip Rev Nanomed Nanobiotechnol.* 5(1):1-18.

IV. Concluding Remarks and Future Perspectives

Although, GBCA are currently used in MRI, recent data suggests a tight association between their use and toxic effects targeting different tissues and organs, including the kidney. This toxicity seems to be a consequence of the slow release of Gd (III) from tissue deposits into the blood stream. Indeed, deposits of Gd (III) have been found in in the brain, bone, skin, liver and kidney. While toxic potential of either Gd (III) and GBCA were already demonstrated in several *in vitro* models, the underlying mechanisms of Gd (III) toxicity are still poorly clarified. This study aimed to disclose the mechanisms involved in the renal toxicity of Gd (III), for that HK-2 cells were used, a well-established cell line of human normal tubular proximal epithelial cells.

We showed that cell viability declined in a concentration- and time-dependent manner after exposure to Gd (III), with estimated ICs eliciting 1 to 50 % of cell death after 24 h of exposure in the micromolar range. Regarding the cellular redox status, Gd (III)-exposed HK-2 cells presented increased oxidative stress, especially at the highest ICs tested. However, our results support the possibility of cells still being able to respond with an upregulation of the antioxidant gene *NRF2*, though this response appears to be insufficient to counteract the overall toxicity of Gd (III).

It was also observed the triggering of mitochondrial dysfunction by Gd (III), which may be derived, at least partially, from the observed oxidative stress. Furthermore, Gd (III) induced cell death by apoptosis, evident already from lower ICs, which appears to switch to necrosis at higher concentrations, which is consistence with the observed energy depletion. Exposure to Gd (III) also appeared to prompt autophagic activation, possibly as an attempt to suppress the exacerbated oxidative damage.

Our data further substantiates a disturbance of the renal lipid metabolism, with accumulation of lipid droplets exposed cells even at the lowest ICs, whose formation may embody a defense mechanism against lipid peroxidation following oxidative damage.

The exposure of HK-2 cells to Gd (III) was also shown to increase the expression of several modulators associated to the development of renal inflammation, tubular hypoxia and fibrosis, and even the regulation of the renal circadian rhythm appears to be targeted by this metal.

In summary, this work shows that Gd (III) has direct nephrotoxic potential, involving multiple cellular and molecular pathways (Figure 3).

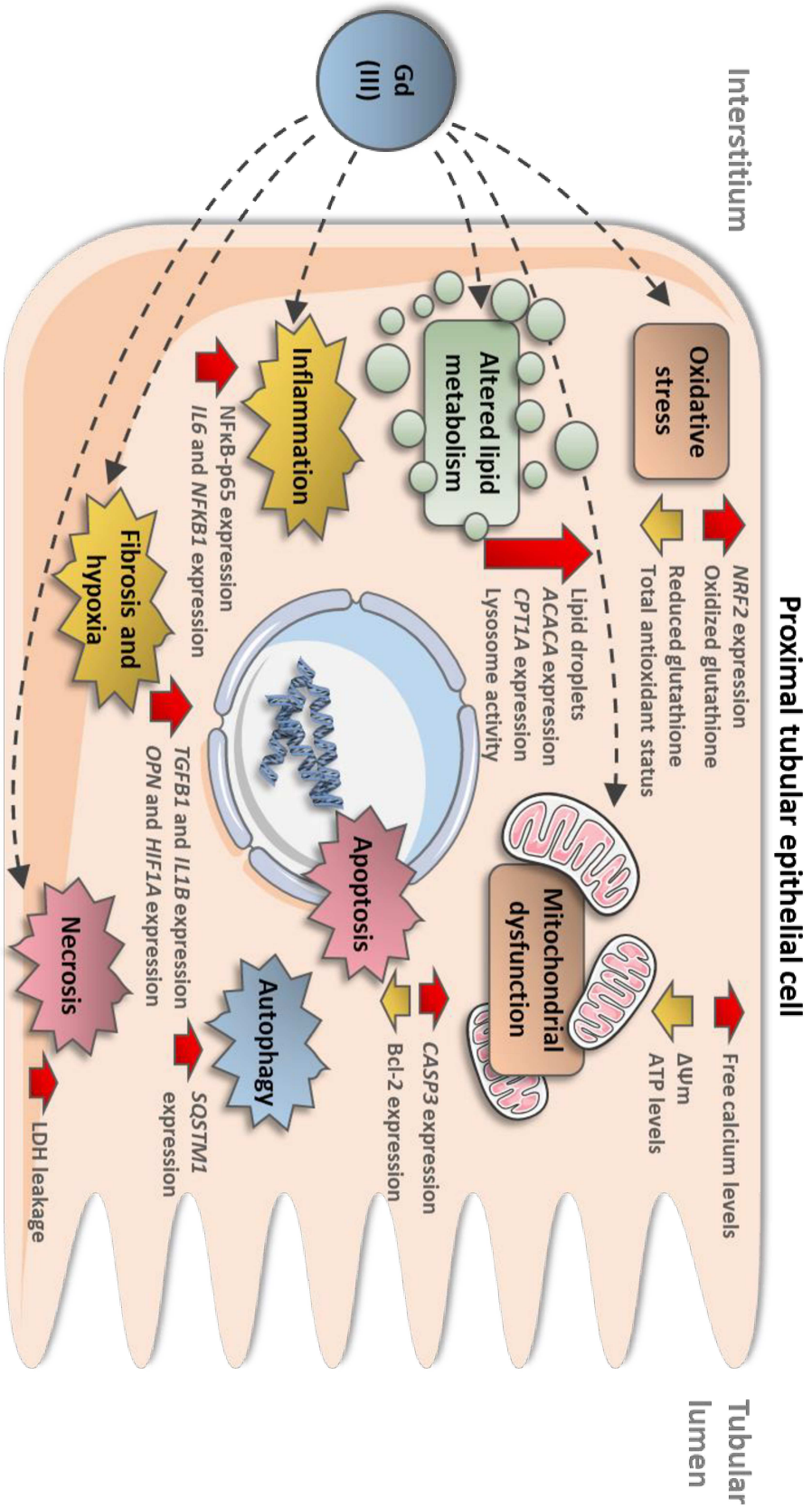


Figure 3: Schematic view of the deleterious effects of gadolinium in the human proximal tubular cells. *ACACA*: acetyl-CoA carboxylase 1; ATP: adenosine triphosphate; Bcl-2: B-cell lymphoma 2; *CASP3*: caspase 3; *CPT1A*: carnitine palmitoyltransferase 1A; *HIF1A*: hypoxia-inducible factor-1 alpha; *IL1B*: interleukin-1 beta; *IL6*: interleukin-6; LDH: lactate dehydrogenase; *OPN*: osteopontin; *NFκB*: nuclear factor-kappa B; *NFKB1*: nuclear factor-kappa B subunit 1; *NRF2*: nuclear factor erythroid-2-related factor 2; *SQSTM1*: sequestosome-1; *TGFβ1*: transforming growth factor beta 1; $\Delta\Psi_m$: mitochondrial membrane potential.

Currently, Gd (III) is the only heavy metal suitable for MRI enhancement, being crucial for diagnosis, staging and monitoring of disease treatment. Nowadays, the use of macrocyclic GBCA, containing more stable chelates of Gd (III), are favoured over linear agents, but even these strong chelates have been associated with Gd (III) retention in the brain and other tissues and with the development of NSF. In our study, the toxicity of uncomplexed Gd (III) was evaluated at concentrations that may or may not be pathophysiologically relevant. It is, thus, of utmost importance to find out how much Gd (III) dechelates from the GBCA currently in use, and which amount of this metal actually accumulates in tissues, and for how long. Also, it appears crucial to identify the pharmacological effects triggered by each type of GBCA, following either single or repeated exposures, and clarify the influence of pre-existing renal dysfunction in these effects. Additionally, the full characterization of the molecular and cellular mechanisms underlying the toxicity of Gd (III) and GBCA at the main target organs, besides the kidney, will also contribute to clarify the actual risks associated to the use of these agents, and guide future research towards the development of safer imaging agents and of potential treatment approaches of adverse effects.

V. References

- Abel, M., Talbot, R. B. Gadolinium oxide inhalation by guinea pigs: a correlative functional and histopathologic study. *J Pharmacol Exp Ther*, 157(1), 207-213, 1967.
- Abraham, J. L., Thakral, C. Tissue distribution and kinetics of gadolinium and nephrogenic systemic fibrosis. *Eur J Radiol*, 66(2), 200-207, 2008.
- Abujudeh, H. H., Kosaraju, V. K., Kaewlai, R. Acute adverse reactions to gadopentetate dimeglumine and gadobenate dimeglumine: experience with 32,659 injections. *AJR Am J Roentgenol*, 194(2), 430-434, 2010.
- Aime, S., Caravan, P. Biodistribution of gadolinium-based contrast agents, including gadolinium deposition. *J Magn Reson Imaging*, 30(6), 1259-1267, 2009.
- Akgun, H., Gonlusen, G., Cartwright, J., Jr., Suki, W. N., Truong, L. D. Are gadolinium-based contrast media nephrotoxic? A renal biopsy study. *Arch Pathol Lab Med*, 130(9), 1354-1357, 2006.
- Altun, E., Semelka, R. C., Cakit, C. Nephrogenic systemic fibrosis and management of high-risk patients. *Acad Radiol*, 16(7), 897-905, 2009.
- Angeli, J. K., Ramos, D. B., Casali, E. A., Souza, D. O., Sarkis, J. J., Stefanon, I., Vassallo, D. V., Furstenau, C. R. Gadolinium increases the vascular reactivity of rat aortic rings. *Braz J Med Biol Res*, 44(5), 445-452, 2011.
- Bajaj, P., Chowdhury, S. K., Yucha, R., Kelly, E. J., Xiao, G. Emerging Kidney Models to Investigate Metabolism, Transport, and Toxicity of Drugs and Xenobiotics. *Drug Metab Dispos*, 46(11), 1692-1702, 2018.
- Ball, R. A., Van Gelder, G. Chronic toxicity of gadolinium oxide for mice following exposure by inhalation. *Arch Environ Health*, 13(5), 601-608, 1966.
- Behzadi, A. H., Zhao, Y., Farooq, Z., Prince, M. R. Immediate Allergic Reactions to Gadolinium-based Contrast Agents: A Systematic Review and Meta-Analysis. *Radiology*, 286(2), 471-482, 2018.
- Blasco-Perrin, H., Glaser, B., Pienkowski, M., Peron, J. M., Payen, J. L. Gadolinium induced recurrent acute pancreatitis. *Pancreatology*, 13(1), 88-89, 2013.

Bose, C., Megyesi, J. K., Shah, S. V., Hiatt, K. M., Hall, K. A., Karaduta, O., Swaminathan, S. Evidence Suggesting a Role of Iron in a Mouse Model of Nephrogenic Systemic Fibrosis. *PLoS One*, 10(8), e0136563, 2015.

Braga, F. S., Vera, Y. M. Separação de gadolínio e európio em meio clorídrico pela técnica de extração por solventes. Paper presented at the XXVII Encontro Nacional de Tratamento de Minérios e Metalurgia Extrativa. Belém 2017.

Broome, D. R. Nephrogenic systemic fibrosis associated with gadolinium based contrast agents: a summary of the medical literature reporting. *Eur J Radiol*, 66(2), 230-234, 2008.

Broome, D. R., Girguis, M. S., Baron, P. W., Cottrell, A. C., Kjellin, I., Kirk, G. A. Gadodiamide-associated nephrogenic systemic fibrosis: why radiologists should be concerned. *AJR Am J Roentgenol*, 188(2), 586-592, 2007.

Burgess, A. E. Contrast effects of a gadolinium filter. *Med Phys*, 8(2), 203-209, 1981.

Bussi, S., Coppo, A., Botteron, C., Fraimbault, V., Fanizzi, A., De Laurentiis, E., Colombo Serra, S., Kirchin, M. A., Tedoldi, F., Maisano, F. Differences in gadolinium retention after repeated injections of macrocyclic MR contrast agents to rats. *J Magn Reson Imaging*, 47(3), 746-752, 2018.

Bussi, S., Coppo, A., Celeste, R., Fanizzi, A., Fringuello Mingo, A., Ferraris, A., Botteron, C., Kirchin, M. A., Tedoldi, F., Maisano, F. Macrocyclic MR contrast agents: evaluation of multiple-organ gadolinium retention in healthy rats. *Insights Imaging*, 11(1), 11, 2020.

Caillé, J. M., Lemanceau, B., Bonnemain, B. Gadolinium as a contrast agent for NMR. *Am J Neuroradiol*, 4(5), 1041-1042, 1983.

Caravan, P., Ellison, J. J., McMurry, T. J., Lauffer, R. B. Gadolinium(III) Chelates as MRI Contrast Agents: Structure, Dynamics, and Applications. *Chem Rev*, 99(9), 2293-2352, 1999.

Carr, D. H., Brown, J., Bydder, G. M., Steiner, R. E., Weinmann, H. J., Speck, U., Hall, A. S., Young, I. R. Gadolinium-DTPA as a contrast agent in MRI: initial clinical experience in 20 patients. *AJR Am J Roentgenol*, 143(2), 215-224, 1984.

Chen, R., Ling, D., Zhao, L., Wang, S., Liu, Y., Bai, R., Baik, S., Zhao, Y., Chen, C., Hyeon, T. Parallel Comparative Studies on Mouse Toxicity of Oxide Nanoparticle- and Gadolinium-Based T1 MRI Contrast Agents. *ACS Nano*, 9(12), 12425-12435, 2015.

Choi, J. W., Moon, W. J. Gadolinium Deposition in the Brain: Current Updates. *Korean J Radiol*, 20(1), 134-147, 2019.

Clases, D., Fingerhut, S., Jeibmann, A., Sperling, M., Doble, P., Karst, U. LA-ICP-MS/MS improves limits of detection in elemental bioimaging of gadolinium deposition originating from MRI contrast agents in skin and brain tissues. *J Trace Elem Med Biol*, 51, 212-218, 2019.

Cohan, R. H., Leder, R. A., Herzberg, A. J., Hedlund, L. W., Wheeler, C. T., Beam, C. A., Nadel, S. N., Dunnick, N. R. Extravascular toxicity of two magnetic resonance contrast agents. Preliminary experience in the rat. *Invest Radiol*, 26(3), 224-226, 1991.

Corot, C., Idee, J. M., Hentsch, A. M., Santus, R., Mallet, C., Goulas, V., Bonnemain, B., Meyer, D. Structure-activity relationship of macrocyclic and linear gadolinium chelates: investigation of transmetallation effect on the zinc-dependent metalloproteinase angiotensin-converting enzyme. *J Magn Reson Imaging*, 8(3), 695-702, 1998.

Damme, N. M., Fernandez, D. P., Wang, L. M., Wu, Q., Kirk, R. A., Towner, R. A., McNally, J. S., Hoffman, J. M., Morton, K. A. Analysis of retention of gadolinium by brain, bone, and blood following linear gadolinium-based contrast agent administration in rats with experimental sepsis. *Magn Reson Med*, 83(6), 1930-1939, 2020.

de Haen, C. Conception of the first magnetic resonance imaging contrast agents: a brief history. *Top Magn Reson Imaging*, 12(4), 221-230, 2001.

Dekkers, I. A., Roos, R., van der Molen, A. J. Gadolinium retention after administration of contrast agents based on linear chelators and the recommendations of the European Medicines Agency. *Eur Radiol*, 28(4), 1579-1584, 2018.

Del Galdo, F., Wermuth, P. J., Addya, S., Fortina, P., Jimenez, S. A. NF κ B activation and stimulation of chemokine production in normal human macrophages by the gadolinium-based magnetic resonance contrast agent Omniscan: possible role in the pathogenesis of nephrogenic systemic fibrosis. *Ann Rheum Dis*, 69(11), 2024-2033, 2010.

Do, C., Barnes, J. L., Tan, C., Wagner, B. Type of MRI contrast, tissue gadolinium, and fibrosis. *Am J Physiol Renal Physiol*, 307(7), F844-855, 2014.

Do, C., DeAguero, J., Brearley, A., Trejo, X., Howard, T., Escobar, G. P., Wagner, B. Gadolinium-Based Contrast Agent Use, Their Safety, and Practice Evolution. *Kidney360*, 1(6), 561-568, 2020.

Elias Jr, J., Santos, A. C., Koenigkam-Santos, M., Nogueira-Barbosa, M. H., Muglia, V. F. Complications from the use of intravenous gadoliniumbased contrast agents for magnetic resonance imaging. *Radiol Bras*, 41(4), 263-267, 2008.

Elmstahl, B., Nyman, U., Leander, P., Chai, C. M., Golman, K., Bjork, J., Almen, T. Gadolinium contrast media are more nephrotoxic than iodine media. The importance of osmolality in direct renal artery injections. *Eur Radiol*, 16(12), 2712-2720, 2006.

Ergun, I., Keven, K., Uruc, I., Ekmekci, Y., Canbakan, B., Erden, I., Karatan, O. The safety of gadolinium in patients with stage 3 and 4 renal failure. *Nephrol Dial Transplant*, 21(3), 697-700, 2006.

Evans, C. H. Biochemistry of the Lanthanides. Springer US, 1990.

FDA. FDA evaluating the risk of brain deposits with repeated use of gadolinium-based contrast agents for magnetic resonance imaging (MRI). Retrieved from FDA evaluating the risk of brain deposits with repeated use of gadolinium-based contrast agents for magnetic resonance imaging (MRI), 2015.

Franckenberg, S., Berger, F., Schaerli, S., Ampanozi, G., Thali, M. Fatal anaphylactic reaction to intravenous gadobutrol, a gadolinium-based MRI contrast agent. *Radiol Case Rep*, 13(1), 299-301, 2018.

Frenzel, T., Lengsfeld, P., Schirmer, H., Hutter, J., Weinmann, H. J. Stability of gadolinium-based magnetic resonance imaging contrast agents in human serum at 37 degrees C. *Invest Radiol*, 43(12), 817-828, 2008.

Granata, V., Cascella, M., Fusco, R., dell'Aprovitola, N., Catalano, O., Filice, S., Schiavone, V., Izzo, F., Cuomo, A., Petrillo, A. Immediate Adverse Reactions to Gadolinium-Based MR Contrast Media: A Retrospective Analysis on 10,608 Examinations. *Biomed Res Int*, 2016, 3918292, 2016.

Grobner, T. Gadolinium--a specific trigger for the development of nephrogenic fibrosing dermopathy and nephrogenic systemic fibrosis? *Nephrol Dial Transplant*, 21(4), 1104-1108, 2006.

Haley, T. J., Raymond, K., Komesu, N., Upham, H. C. Toxicological and pharmacological effects of gadolinium and samarium chlorides. *Br J Pharmacol Chemother*, 17, 526-532, 1961.

Hao, D., Ai, T., Goerner, F., Hu, X., Runge, V. M., Tweedle, M. MRI contrast agents: basic chemistry and safety. *J Magn Reson Imaging*, 36(5), 1060-1071, 2012.

Haylor, J., Vickers, M. E., Morcos, S. K. Interference of gadolinium-based contrast agents with the measurement of serum creatinine by the Jaffe reaction. *Br J Radiol*, 82(977), 438-439, 2009.

Heinrich, M. C., Kuhlmann, M. K., Kohlbacher, S., Scheer, M., Grgic, A., Heckmann, M. B., Uder, M. Cytotoxicity of iodinated and gadolinium-based contrast agents in renal tubular cells at angiographic concentrations: in vitro study. *Radiology*, 242(2), 425-434, 2007.

High, W. A., Ayers, R. A., Cowper, S. E. Gadolinium is quantifiable within the tissue of patients with nephrogenic systemic fibrosis. *J Am Acad Dermatol*, 56(4), 710-712, 2007.

Idee, J. M., Fretellier, N., Robic, C., Corot, C. The role of gadolinium chelates in the mechanism of nephrogenic systemic fibrosis: A critical update. *Crit Rev Toxicol*, 44(10), 895-913, 2014.

Infarmed. Circular informativa N.º 100/CD/550.20.001 Retrieved from infarmed.pt/documents/15786/1878974/Restrição+da+utilização+de+agentes+de+contraste+de+estrutura+linear+que+contêm+gadolinio/44dac3d1-48c6-4a51-a0f1-431dd57b3a64, 2017.

Kalogeromitros, D. C., Makris, M. P., Aggelides, X. S., Spanoudaki, N., Gregoriou, S. G., Avgerinou, G., Rigopoulos, D. G. Anaphylaxis to gadobenate dimeglumine (Multihance): a case report. *Int Arch Allergy Immunol*, 144(2), 150-154, 2007.

Kanal, E., Tweedle, M. F. Residual or retained gadolinium: practical implications for radiologists and our patients. *Radiology*, 275(3), 630-634, 2015.

Kanda, T., Ishii, K., Kawaguchi, H., Kitajima, K., Takenaka, D. High signal intensity in the dentate nucleus and globus pallidus on unenhanced T1-weighted MR images: relationship with increasing cumulative dose of a gadolinium-based contrast material. *Radiology*, 270(3), 834-841, 2014.

Kay, J., Bazari, H., Avery, L. L., Koreishi, A. F. Case records of the Massachusetts General Hospital. Case 6-2008. A 46-year-old woman with renal failure and stiffness of the joints and skin. *N Engl J Med*, 358(8), 827-838, 2008.

Lancelot, E. Revisiting the Pharmacokinetic Profiles of Gadolinium-Based Contrast Agents: Differences in Long-Term Biodistribution and Excretion. *Invest Radiol*, 51(11), 691-700, 2016.

Lancelot, E., Desche, P. Gadolinium Retention as a Safety Signal: Experience of a Manufacturer. *Invest Radiol*, 55(1), 20-24, 2020.

Li, A., Wong, C. S., Wong, M. K., Lee, C. M., Au Yeung, M. C. Acute adverse reactions to magnetic resonance contrast media--gadolinium chelates. *Br J Radiol*, 79(941), 368-371, 2006.

Liu, H., Yuan, L., Yang, X., Wang, K. La(3+), Gd(3+) and Yb(3+) induced changes in mitochondrial structure, membrane permeability, cytochrome c release and intracellular ROS level. *Chem Biol Interact*, 146(1), 27-37, 2003.

Lohrke, J., Frisk, A. L., Frenzel, T., Schockel, L., Rosenbruch, M., Jost, G., Lenhard, D. C., Sieber, M. A., Nischwitz, V., Kuppers, A., Pietsch, H. Histology and Gadolinium Distribution in the Rodent Brain After the Administration of Cumulative High Doses of Linear and Macrocyclic Gadolinium-Based Contrast Agents. *Invest Radiol*, 52(6), 324-333, 2017.

Lord, M. L., Chettle, D. R., Grafe, J. L., Noseworthy, M. D., McNeill, F. E. Observed Deposition of Gadolinium in Bone Using a New Noninvasive in Vivo Biomedical Device: Results of a Small Pilot Feasibility Study. *Radiology*, 287(1), 96-103, 2018.

McDonald, J. S., Hunt, C. H., Kolbe, A. B., Schmitz, J. J., Hartman, R. P., Maddox, D. E., Kallmes, D. F., McDonald, R. J. Acute Adverse Events Following Gadolinium-based Contrast Agent Administration: A Single-Center Retrospective Study of 281 945 Injections. *Radiology*, 292(3), 620-627, 2019.

McKoy, J. M., Laumann, A., Samaras, A., Lacouture, M., West, D., Raisch, D., Obadina, E., Fajolu, O., Reilly, L., Bennett, C. L. Gadolinium-associated nephrogenic systemic fibrosis. *Community Oncol*, 5(6), 325-326, 2008.

Mercantepe, T., Tumkaya, L., Celiker, F. B., Topal Suzan, Z., Cinar, S., Akyildiz, K., Mercantepe, F., Yilmaz, A. Effects of gadolinium-based MRI contrast agents on liver tissue. *J Magn Reson Imaging*, 48(5), 1367-1374, 2018.

Mundim, J. S., Lorena, S. d. C., Abensur, H., Elias, R. M., Moysés, R. M. A., Castro, M. C. M., Romão Jr, J. E. Fibrose sistêmica nefrogênica: uma complicação grave do uso do gadolínio em pacientes com insuficiência renal. *Rev Assoc Med Bras*, 55(2), 220-225, 2009.

Murata, N., Gonzalez-Cuyar, L. F., Murata, K., Fligner, C., Dills, R., Hippe, D., Maravilla, K. R. Macrocyclic and Other Non-Group 1 Gadolinium Contrast Agents Deposit Low Levels of Gadolinium in Brain and Bone Tissue: Preliminary Results From 9 Patients With Normal Renal Function. *Invest Radiol*, 51(7), 447-453, 2016.

Newton, B. B., Jimenez, S. A. Mechanism of NSF: New evidence challenging the prevailing theory. *J Magn Reson Imaging*, 30(6), 1277-1283, 2009.

Niendorf, H. P., Seifert, W. Serum iron and serum bilirubin after administration of Gd-DTPA-dimeglumine. A pharmacologic study in healthy volunteers. *Invest Radiol*, 23 Suppl 1, S275-280, 1988.

Okada, E., Yamanaka, M., Ishikawa, O. New insights into the mechanism of abnormal calcification in nephrogenic systemic fibrosis - gadolinium promotes calcium deposition of mesenchymal stem cells and dermal fibroblasts. *J Dermatol Sci*, 62(1), 58-63, 2011.

Othersen, J. B., Maize, J. C., Woolson, R. F., Budisavljevic, M. N. Nephrogenic systemic fibrosis after exposure to gadolinium in patients with renal failure. *Nephrol Dial Transplant*, 22(11), 3179-3185, 2007.

Otnes, S., Fogh-Andersen, N., Romsing, J., Thomsen, H. S. Analytical Interference by Contrast Agents in Biochemical Assays. *Contrast Media Mol Imaging*, 2017, 1323802, 2017.

Perazella, M. A. Current status of gadolinium toxicity in patients with kidney disease. *Clin J Am Soc Nephrol*, 4(2), 461-469, 2009.

Proctor, K. A., Rao, L. V., Roberts, W. L. Gadolinium magnetic resonance contrast agents produce analytic interference in multiple serum assays. *Am J Clin Pathol*, 121(2), 282-292, 2004.

Rogosnitzky, M., Branch, S. Gadolinium-based contrast agent toxicity: a review of known and proposed mechanisms. *Biometals*, 29(3), 365-376, 2016.

Rogowska, J., Olkowska, E., Ratajczyk, W., Wolska, L. Gadolinium as a new emerging contaminant of aquatic environments. *Environ Toxicol Chem*, 37(6), 1523-1534, 2018.

Runge, V. M., Schoerner, W., Niendorf, H. P., Laniado, M., Koehler, D., Claussen, C., Felix, R., James, A. E., Jr. Initial clinical evaluation of gadolinium DTPA for contrast-enhanced magnetic resonance imaging. *Magn Reson Imaging*, 3(1), 27-35, 1985.

Sato, T., Ito, K., Tamada, T., Kanki, A., Watanabe, S., Nishimura, H., Tanimoto, D., Higashi, H., Yamamoto, A. Tissue gadolinium deposition in renally impaired rats exposed to different gadolinium-based MRI contrast agents: evaluation with inductively coupled plasma mass spectrometry (ICP-MS). *Magn Reson Imaging*, 31(8), 1412-1417, 2013.

Schieda, N., Blaichman, J. I., Costa, A. F., Glikstein, R., Hurrell, C., James, M., Jabehdar Maralani, P., Shabana, W., Tang, A., Tsampalieros, A., van der Pol, C., Hiremath, S. Gadolinium-Based Contrast Agents in Kidney Disease: Comprehensive Review and Clinical Practice Guideline Issued by the Canadian Association of Radiologists. *Can Assoc Radiol J*, 69(2), 136-150, 2018.

Sherry, A. D., Caravan, P., Lenkinski, R. E. Primer on gadolinium chemistry. *J Magn Reson Imaging*, 30(6), 1240-1248, 2009.

Soloff, E. V., Wang, C. L. Safety of gadolinium-based contrast agents in patients with stage 4 and 5 chronic kidney disease: a radiologist's perspective. *Kidney360*, 1(2), 123-126, 2020.

Swaminathan, S., High, W. A., Ranville, J., Horn, T. D., Hiatt, K., Thomas, M., Brown, H. H., Shah, S. V. Cardiac and vascular metal deposition with high mortality in nephrogenic systemic fibrosis. *Kidney Int*, 73(12), 1413-1418, 2008.

Thakral, C., Abraham, J. L. Gadolinium-induced nephrogenic systemic fibrosis is associated with insoluble Gd deposits in tissues: in vivo transmetallation confirmed by microanalysis. *J Cutan Pathol*, 36(12), 1244-1254, 2009.

Thakral, C., Alhariri, J., Abraham, J. L. Long-term retention of gadolinium in tissues from nephrogenic systemic fibrosis patient after multiple gadolinium-enhanced MRI scans: case report and implications. *Contrast Media Mol Imaging*, 2(4), 199-205, 2007.

Thomsen, H. S. Gadolinium-based contrast media may be nephrotoxic even at approved doses. *Eur Radiol*, 14(9), 1654-1656, 2004.

Uhlig, J., Lucke, C., Vliegenthart, R., Loewe, C., Grothoff, M., Schuster, A., Lurz, P., Jacquier, A., Francone, M., Zapf, A., Schulke, C., Daniel, T., May, M. S., Bremerich, J., Lotz, J., Gutberlet, M., contributors, E. M. R. Acute adverse events in cardiac MR imaging with gadolinium-based contrast agents: results from the European Society of Cardiovascular Radiology (ESCR) MRCT Registry in 72,839 patients. *Eur Radiol*, 29(7), 3686-3695, 2019.

Wagner, B., Drel, V., Gorin, Y. Pathophysiology of gadolinium-associated systemic fibrosis. *Am J Physiol Renal Physiol*, 311(1), F1-F11, 2016.

Wermuth, P. J., Jimenez, S. A. Induction of a type I interferon signature in normal human monocytes by gadolinium-based contrast agents: comparison of linear and macrocyclic agents. *Clin Exp Immunol*, 175(1), 113-125, 2014.

Xia, Q., Feng, X., Huang, H., Du, L., Yang, X., Wang, K. Gadolinium-induced oxidative stress triggers endoplasmic reticulum stress in rat cortical neurons. *J Neurochem*, 117(1), 38-47, 2011.